

TSPYL5 suppresses p53 levels and function by physical interaction with USP7

Mirjam T. Epping^{1,2}, Lars A.T. Meijer³, Oscar Krijgsman^{4,5}, Johannes L. Bos³, Pier Paolo Pandolfi² and René Bernards^{1,6}

We have previously reported a gene expression signature that is a powerful predictor of poor clinical outcome in breast cancer¹. Among the seventy genes in this expression profile is a gene of unknown function: TSPYL5 (TSPY-like 5, also known as KIAA1750). TSPYL5 is located within a small region at chromosome 8q22 that is frequently amplified in breast cancer, which suggests that TSPYL5 has a causal role in breast oncogenesis^{2,3}. Here, we report that high TSPYL5 expression is an independent marker of poor outcome in breast cancer. Mass spectrometric analysis revealed that TSPYL5 interacts with ubiquitin-specific protease 7 (USP7; also known as herpesvirus-associated ubiquitin-specific protease; HAUSP). USP7 is the deubiquitylase for the p53 tumour suppressor⁴ and TSPYL5 reduces the activity of USP7 towards p53, resulting in increased p53 ubiquitylation. We demonstrate that TSPYL5 reduces p53 protein levels and inhibits activation of p53-target genes. Furthermore, expression of TSPYL5 overrides p53-dependent proliferation arrest and oncogene-induced senescence, and contributes to oncogenic transformation in multiple cell-based assays. Our data identify TSPYL5 as a suppressor of p53 function through its interaction with USP7.

The p53 tumour suppressor is essential for cell-cycle arrest and apoptosis after genotoxic stress^{5,6}. p53 is also required for the induction of senescence after oncogene activation, which is considered to be a mechanism to prevent tumourigenesis⁵. One of the major roles of p53 is to activate transcription of a wide range of target genes to exert its cancer prevention function⁷. p53 is tightly regulated, mainly at the level of protein stability, to allow rapid protein accumulation and activation after DNA damage. Homeostatic p53 levels under normal conditions are low owing to the actions of several ubiquitin ligases that mark p53 for ubiquitin-dependent degradation by the 26S proteasome⁸. p53 ubiquitylation is reversible and the deubiquitylase USP7 has been demonstrated to catalyse the removal of ubiquitin chains from p53 (ref. 4). The

p53 network is complex and many factors contribute to the control and activation of this tumour suppressor^{5,6}.

Gene expression profiling has been used to generate gene signatures that can predict the clinical outcome of breast cancers patients^{1,9–11}. These signatures are based on microarray analysis of primary tumours and are predictive of a short interval to distant metastases. The genes in such multi-gene predictors can vary from 2 to over 100, which together form a 'prognostic signature'. The genes that comprise such prognostic signatures represent signalling pathways that are essential for cell cycle, invasion, metastasis and angiogenesis¹. *TSPYL5* is among the genes in the MammaPrint 70-gene prognostic expression signature that predicts clinical outcome of breast cancer¹. *TSPYL5* is a member of the testis-specific protein, Y-encoded-like (TSPY-L) family of genes, whose functions are currently unknown. The genomic location of the *TSPYL5* gene is chromosome 8q22, a region that is frequently amplified in breast cancer (Fig. 1b)^{2,3}. Genomic gain of this region has been detected in 21–27% of primary breast tumour samples and is associated with a higher propensity of metastatic recurrence^{2,3}.

To address the role of *TSPYL5* in breast cancer, we investigated whether *TSPYL5* is an independent marker of disease outcome using a consecutive series of 295 primary breast carcinomas with long clinical follow-up for which microarray gene expression data are publicly available⁹. We randomly split this series into a training set of 152 tumours and a validation set of 143. Using the training set, we determined the expression level of *TSPYL5* that yielded the largest difference in survival between the *TSPYL5*^{high} and *TSPYL5*^{low} groups. We then investigated whether this *TSPYL5* expression threshold was also prognostic for disease outcome in the validation set. Figure 1a indicates that high *TSPYL5* mRNA expression levels are correlated with shortened distant metastasis-free survival in the validation set ($P = 0.0063$; $n = 143$), indicating that *TSPYL5* as a single marker is prognostic for disease outcome in breast cancer.

Gene expression analysis has allowed the identification of molecular subtypes of breast carcinoma with distinct clinical outcomes¹². To investigate whether *TSPYL5* was differentially expressed among these molecular

¹Division of Molecular Carcinogenesis, Centre for Biomedical Genetics and Cancer Genomics Centre, Netherlands Cancer Institute, Plesmanlaan 121, 1066 CX Amsterdam, Netherlands. ²Cancer Genetics Program, Beth Israel Deaconess Cancer Center, Departments of Medicine and Pathology, Beth Israel Deaconess Medical Center, Harvard Medical School, Boston, MA 02215, USA. ³Department of Physiological Chemistry, Centre for Biomedical Genetics and Cancer Genomics Centre, University Medical Center Utrecht, Heidelberglaan 100, 3584 CX Utrecht, Netherlands. ⁴Agendia BV, Science Park 406, 1098 XH Amsterdam, Netherlands. ⁵Department of Pathology, VU Medical Center, De Boelelaan 1117, 1081 HV Amsterdam, Netherlands. ⁶Correspondence should be addressed to R.B. (e-mail: r.bernards@nki.nl)

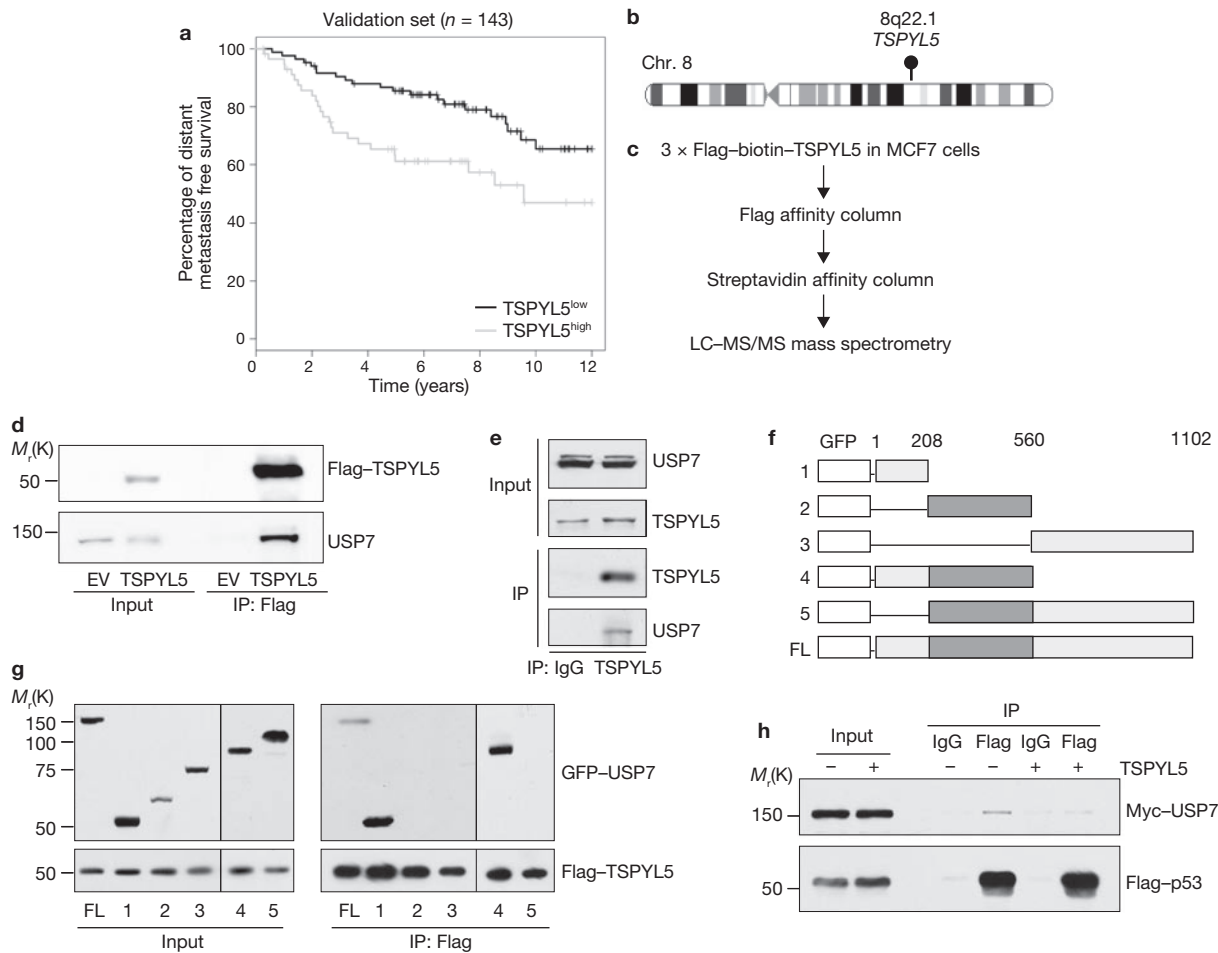


Figure 1 TSPYL5 is a poor-prognosis marker in breast cancer and binds to USP7. **(a)** Kaplan–Meier plot of distant metastasis-free survival of breast cancer patients ($n = 143$) with low ($n = 84$) or high ($n = 59$) *TSPYL5* gene expression in the validation set. **(b)** Schematic representation of *TSPYL5* location on chromosome 8q22, a region of recurrent amplification in breast cancer. **(c)** Summary of protocol used to purify TSPYL5 from MCF7 cells with stable expression of 3 × Flag-biotin-TSPYL5. Mass spectrometric analysis identified USP7 as a TSPYL5-binding protein. **(d)** MCF7 cells were infected with retrovirus encoding Flag-TSPYL5 or empty vector (EV; as a control). Cell lysates were immunoprecipitated with anti-Flag antibodies and analysed by western blot using anti-USP7 and anti-Flag antibodies. **(e)** TSPYL5 was

immunoprecipitated from PC3 cells with an antibody against TSPYL5 and the western blots were stained with anti-USP7 and anti-TSPYL5 antibodies. IgG; immunoglobulin G. **(f)** Schematic representation of USP7 domains fused to GFP that were used for the interaction analysis in **g** (FL; full-length). **(g)** Lysates of cells transfected with plasmids encoding Flag-TSPYL5 and the indicated GFP-USP7 domains (as defined in **f**) were immunoprecipitated with anti-Flag antibody and analysed by western blotting. **(h)** Lysates of cells transfected with plasmids encoding Flag-p53, Myc-USP7 and either TSPYL5 or empty vector were immunoprecipitated with anti-Flag antibody and analysed by western blotting. Uncropped images of blots are shown in Supplementary Information, Fig. S6.

subtypes, we determined the subtypes of the 295 breast cancers¹³ and measured *TSPYL5* expression. *TSPYL5* expression was highest in basal-like breast cancers (Supplementary Information, Fig. S1). Consistent with the hypothesis that *TSPYL5* is a poor prognosis marker, basal-like tumours have the worst prognosis among the molecular subtypes¹².

To gain insight into its function, we searched for proteins that interact with TSPYL5 in MCF7 human breast cancer cells that had 8q22 amplification. We expressed a tagged (3 × Flag-biotin) TSPYL5 protein in these cells and purified TSPYL5-containing protein complexes using a tandem affinity purification method (Fig. 1c). TSPYL5-associated proteins were identified by liquid chromatography mass spectrometry/mass spectrometry (LC-MS/MS; see Methods). One of the proteins that was present in purified TSPYL5 complexes, but not in control purifications, was USP7 (Supplementary Information, Fig. S2). Given the known function of USP7 as the deubiquitylating enzyme (deubiquitylase) for p53

(ref. 4), we focused our attention on USP7 as an interactor of TSPYL5. We first confirmed the physical interaction between Flag-TSPYL5 and endogenous USP7 in MCF7 breast cancer cells and in primary human fibroblasts (Fig. 1d and Supplementary Information, Fig. S3a). We also observed an interaction between endogenous USP7 and endogenous TSPYL5 (Fig. 1e). USP7 contains a central catalytic core domain and amino-terminal and carboxy-terminal domains, which were tested separately for their ability to bind TSPYL5. In immunoprecipitations of cells transfected with various GFP-USP7 domains, TSPYL5 selectively bound to the N-terminal domain (amino-acid residues 1–208) of USP7 (Fig. 1f, g). The USP7 N-terminus was sufficient for the interaction with TSPYL5, which is of interest because this region of USP7 is also required and sufficient for the interaction between USP7 and p53 (Supplementary Information, Fig. S3b)¹⁴. Therefore, it is conceivable that TSPYL5 competes with p53 for binding to the same region of USP7. Consistent with

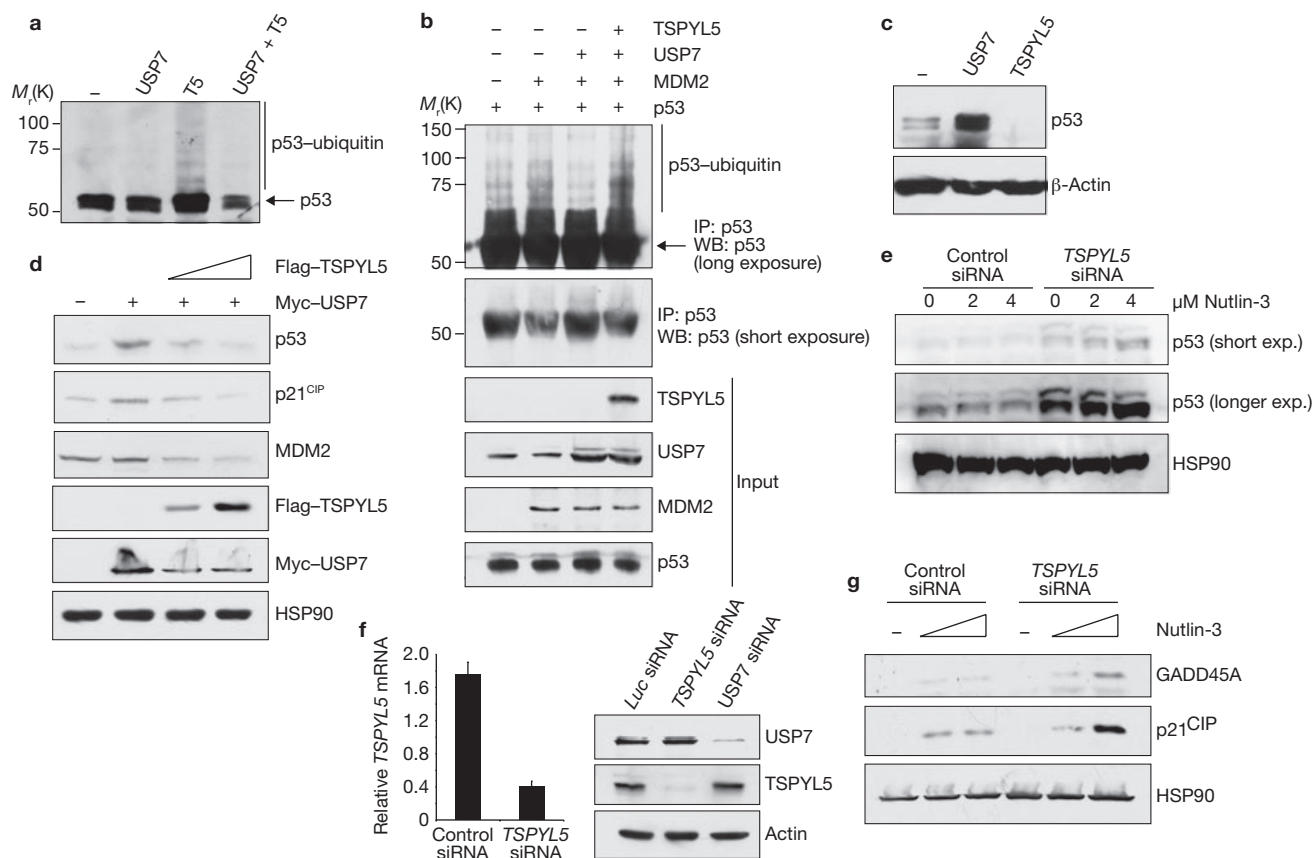


Figure 2 TSPYL5 increases p53 ubiquitylation and suppresses p53 protein levels. (a) PC3 cells were transfected with plasmid encoding p53 and were co-transfected with plasmids encoding USP7, TSPYL5 (T5) or USP7 and TSPYL5. Cells were treated with proteasome inhibitor MG132 and lysates were analysed for p53 ubiquitylation by western blotting with an anti-p53 antibody. (b) Lysates of 293 cells transfected with plasmids encoding the indicated proteins were immunoprecipitated with an anti-p53 antibody and analysed for ubiquitylation by western blotting with an anti-p53 antibody. (c) U2OS cells were transfected with plasmids encoding USP7 or TSPYL5 and lysates were immunoblotted for p53. (d) U2OS cells were transfected with plasmid encoding Myc-USP7 and increasing concentrations of plasmid

encoding Flag-TSPYL5 and were immunoblotted for p53, p21^{CIP} and MDM2. (e) Western blot analysis of MCF7 cells transfected with *TSPYL5* siRNA after treatment with the indicated concentrations of Nutlin-3 for 24 h. Short and longer exposures are shown. (f) Left: qRT-PCR analysis of *TSPYL5* mRNA levels in MCF7 cells transfected with *TSPYL5* siRNA. Relative mRNA levels were normalized to GAPDH (mean \pm s.d.; $n = 3$). Right: western blot analysis of PC3 cells transfected with siRNA against luciferase (Luc siRNA), *TSPYL5* or *USP7*. (g) Western blot analysis of MCF7 cells transfected with *TSPYL5* siRNA, without treatment or after treatment with increasing concentrations of Nutlin-3. Uncropped images of blots are shown in Supplementary Information, Fig. S6.

this hypothesis, we found that the interaction between USP7 and p53 is impaired in the presence of TSPYL5 (Fig. 1h).

To determine how the interaction between TSPYL5 and USP7 affects p53 ubiquitylation, we expressed exogenous *TSPYL5* and treated the cells with the proteasome inhibitor MG132 (CBZ-LLL) to allow ubiquitylated species of p53 to accumulate. Expression of *TSPYL5* increased ubiquitylation of p53, but co-expression of USP7 neutralized this effect (Fig. 2a and Supplementary Information, Fig. S3c). The effects of USP7 on p53 are complex, as USP7 also interacts with MDM2, the ubiquitin ligase for p53 (refs 15, 16). To investigate how these effects converged on p53 ubiquitylation, we co-expressed p53, MDM2, USP7 and *TSPYL5* and studied p53 ubiquitylation. Figure 2b indicates that *TSPYL5* also increased ubiquitylation of p53 in the presence of MDM2. This observation suggests that *TSPYL5* functions primarily as an inhibitor of the deubiquitylation of p53 by USP7. Given this finding, expression of *TSPYL5* would be predicted to lead to a reduction in p53 protein levels. Indeed, transfection of plasmids expressing *TSPYL5* into U2OS cells, which have wild-type p53, caused a significant decrease in endogenous p53 protein levels (Fig. 2c). As expected, USP7 expression increased steady-state p53 levels (Fig. 2c). *TSPYL5* decreased

p53 protein levels in a dose-dependent manner in the presence of USP7, and similarly suppressed the levels of the p53 downstream targets p21^{CIP} and MDM2 (Fig. 2d). To test if the effect of *TSPYL5* on p53 was dependent on USP7, we expressed *TSPYL5* in cells with *USP7* RNA interference (RNAi). After treatment with the DNA damage-inducing drug cisplatin to stabilize p53, the reduction in p53 levels through *TSPYL5* expression were again seen, but not in cells with *USP7* knockdown (Supplementary Information, Fig. S4a). This indicates that *TSPYL5* inhibits p53 stabilization in an USP7-dependent manner.

We tested the effect of *TSPYL5* depletion using siRNA (Fig. 2f), and found that endogenous p53 was increased in MCF7 cells with knockdown of *TSPYL5* (Fig. 2e and Supplementary Information, Fig. S4c). Nutlin-3 is a small molecule drug that disrupts the physical interaction between p53 and MDM2, which causes activation of p53 function¹⁷. Exposure of *TSPYL5*-knockdown cells to increasing concentrations of Nutlin-3 caused a further increase in p53 protein levels (Fig. 2e). Consequently, the p53-targets p21^{CIP} and GADD45A were induced further by *TSPYL5* knockdown on treatment with Nutlin-3 (Fig. 2g). The levels of MDM2 were not affected under these conditions (Supplementary Information,

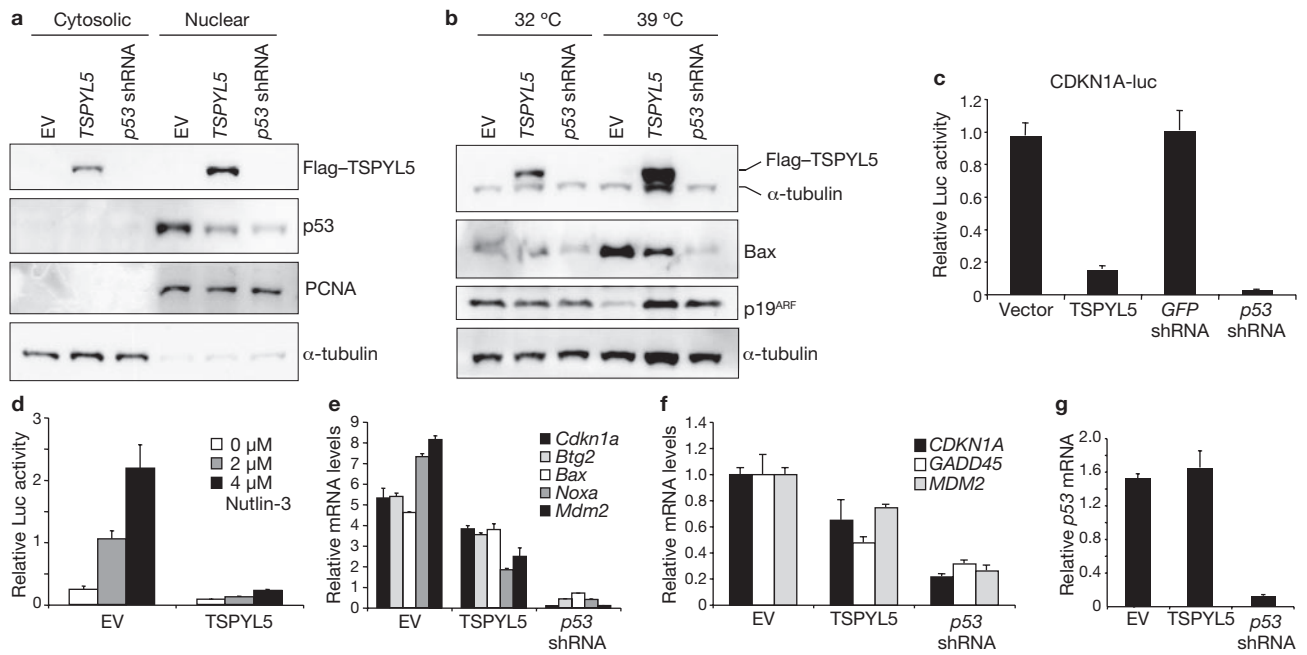


Figure 3 TSPYL5 inhibits p53 transactivation and target gene transcription. (a) Cytosolic and nuclear fractionation of *ST.HdhQ111* cells that were infected with retrovirus encoding Flag-TSPYL5, empty vector or p53 shRNA at the restrictive temperature of 39 °C. (b) Western blot analysis of *ST.HdhQ111* cells cultured at 32 °C or 39 °C. (c) *CDKN1A*-promoter luciferase assay in U2OS cells transfected with plasmid encoding TSPYL5 or shRNA against GFP or p53 (mean \pm s.d.; $n = 3$). (d) *PIG3*-luciferase reporter assay for p53 transactivation in U2OS cells transfected with plasmid encoding TSPYL5 after treatment with the indicated concentrations of

Nutlin-3 for 24 h (mean \pm s.d.; $n = 3$). (e) qRT-PCR analysis of p53 target genes in *ST.HdhQ111* cells, infected with empty vector, retrovirus encoding TSPYL5 or p53 shRNA, at 39 °C. Relative mRNA levels were normalized to β -actin (mean \pm s.d.; $n = 3$). (f, g) qRT-PCR analysis of p53 target genes (f) and p53 mRNA (g) in human BJ fibroblasts with an inducible RAS^{V12}-ER, after treatment with tamoxifen to activate RAS^{V12}. The cells were infected with retrovirus encoding Flag-TSPYL5, empty vector or p53 shRNA. Relative mRNA levels were normalized to β -actin (mean \pm s.d.; $n = 3$). Uncropped images of blots are shown in Supplementary Information, Fig. S6.

Fig. S3d). MCF7 cells with *TSPYL5* RNAi had higher levels of p53 after treatment with cisplatin than did control cells, and had increased PARP cleavage, indicative of apoptosis (Supplementary Information, Fig. S4d, g). We also observed that *TSPYL5* RNAi increased the abundance of p53 after treatment with cisplatin in ZR75-1 breast cancer cells, another cell line that carries the 8q22 amplicon (Supplementary Information, Fig. S4e). Together, these data indicate that TSPYL5 suppresses p53 protein levels by increasing ubiquitin-mediated proteolysis. Furthermore, the finding that TSPYL5 affects p53 also in the presence of Nutlin-3 and cisplatin, two drugs that disrupt the p53-MDM2 interaction, suggest that the observed effects of TSPYL5 on p53 are not mediated indirectly through MDM2. Consistent with this, knockdown of TSPYL5 also increased p53 levels in HeLa cells, in which the HPV E6-associated protein E6AP serves as the main p53 ubiquitin ligase, instead of MDM2 (Supplementary Information, Fig. S4f)¹⁸.

To further investigate the effects of TSPYL5 on p53 function, we stably expressed *TSPYL5* in *ST.HdhQ111* cells: primary mouse neuronal cells conditionally immortalized by a temperature-sensitive mutant of SV40 large T antigen¹⁹. *ST.HdhQ111* cells proliferate rapidly at the permissive temperature (32 °C), but enter into a p53-dependent senescence-like arrest when shifted to the non-permissive temperature (39 °C)¹⁹. On shift to the non-permissive temperature, we observed a reduced abundance of p53 protein in cells expressing *TSPYL5*, compared with control cells infected with empty vector (Fig. 3a). Consequently, the induction of the p53 target gene *Bax* was suppressed by expression of *TSPYL5* (Fig. 3b). TSPYL5 was localized in the nucleus and in the cytosol,

whereas p53 remained strictly nuclear (Fig. 3a). The levels of p19^{ARF} protein were low in control cells and high in both TSPYL5-expressing cells and cells with shRNA against p53 (Fig. 3b), consistent with the known reciprocal relation between p53 and p19^{ARF} (ref. 20). Hence, TSPYL5 functions downstream of p19^{ARF}, which is consistent with the hypothesis that TSPYL5 acts through USP7 to suppress p53.

To test p53 transcriptional activity, we used a *CDKN1A* promoter-driven luciferase construct, one of the best-characterized p53 target genes. TSPYL5 strongly inhibited p53-dependent transcription of both this reporter (Fig. 3c) and a second p53-dependent luciferase reporter²¹ (*PIG3*-luciferase, Supplementary Information, Fig. S5a). Moreover, the mRNA levels of five *bona fide* p53 target genes (measured by quantitative reverse transcriptase PCR; qRT-PCR) were lower in TSPYL5-*ST.HdhQ111* cells at 39 °C than in control cells (Fig. 3e). TSPYL5 also reduced p53 target gene mRNA levels in human fibroblasts with an activated p53 response owing to expression of a RAS^{V12} oncogene (Fig. 3f). Importantly, the level of p53 mRNA was not affected by TSPYL5, supporting the hypothesis that suppression of p53 by TSPYL5 is post-transcriptional (Fig. 3g). When the p53 reporter gene assays were repeated in the presence of the Nutlin-3, we found that TSPYL5 still strongly inhibited *PIG3*-luciferase activity (Fig. 3d). As Nutlin-3 is an inhibitor of MDM2, this result again suggests that the TSPYL5-USP7 complex acts directly on p53 and not indirectly through an effect on MDM2. Consistent with this, TSPYL5 could strongly suppress the *PIG3*-luciferase reporter in cells in which MDM2 had been removed by RNAi (Supplementary Information, Fig. S5b). In addition, TSPYL5

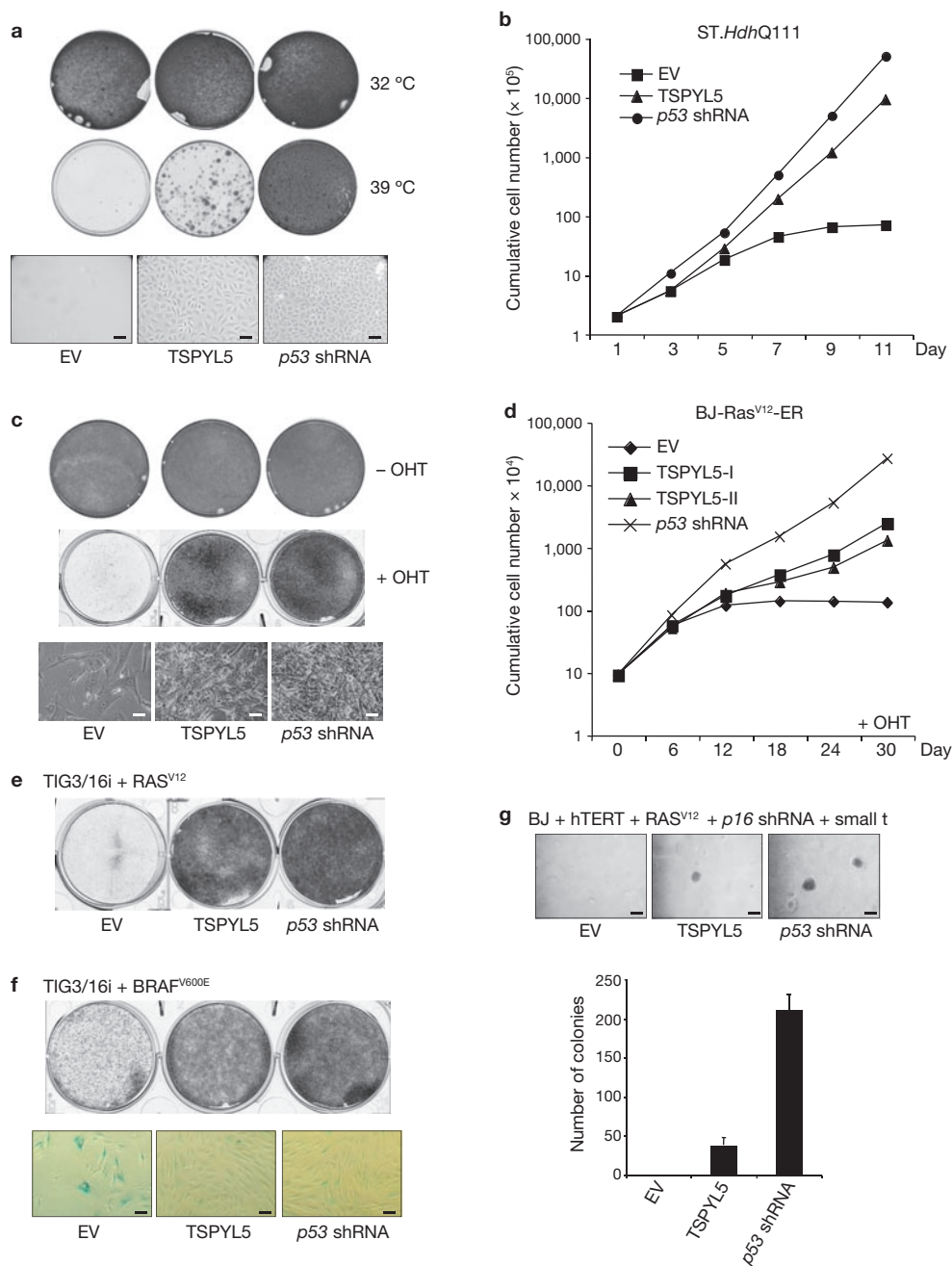


Figure 4 TSPYL5 inhibits oncogene-induced senescence and allows transformation. **(a)** ST.HdhQ111 cells were infected with empty vector, retrovirus encoding Flag-TSPYL5 or p53 shRNA and were cultured at 32 °C or 39 °C. Top: culture dishes were stained with Coomassie blue and photographed after 3 weeks. Bottom: Phase-contrast microscopy images of ST.HdhQ111 cells proliferating at 39 °C. Scale bar, 10 μ m. **(b)** Proliferation of ST.HdhQ111 cells at 39 °C. **(c)** BJ fibroblasts with an inducible RAS^{V12}-ER were infected with empty vector, retrovirus encoding Flag-TSPYL5 or p53 shRNA, and were treated with tamoxifen (OHT) to activate RAS^{V12}. Top: culture dishes were stained with Coomassie blue and photographed after 3 weeks. Bottom: Phase-contrast microscopy images of BJ-RAS^{V12}-ER cells proliferating in the presence of tamoxifen. Scale bar, 10 μ m. **(d)** Proliferation

of BJ-RAS^{V12}-ER cells in the continuous presence of tamoxifen. **(e)** TIG3/16i cells infected with empty vector, retrovirus encoding Flag-TSPYL5 or p53 shRNA and were subsequently infected with RAS^{V12} retrovirus. **(f)** TIG3/16i cells were infected with empty vector, retrovirus encoding Flag-TSPYL5, or p53 shRNA and were subsequently infected with BRAF^{V600E} retrovirus. Top: culture dishes were stained with Coomassie blue and photographed after 3 weeks. Bottom: microscopy images of cells stained for the senescence marker acidic β -galactosidase. Scale bar, 10 μ m. **(g)** Soft agar transformation assay of BJ cells with stable expression of hTERT, RAS^{V12}, p16 shRNA, small t antigen and TSPYL5 or p53 shRNA (empty vector was used as a control; data are means \pm s.d.; $n = 3$). Top: photographs of colony formation. Scale bar, 500 μ m. Bottom: quantification of colonies formed.

repressed PIG3-luciferase induction by treatment of cells with cisplatin (Supplementary Information, Fig. S5c). Together, these data indicate that MDM2 is not required for the effects of TSPYL5 on p53.

To test the functional consequences of TSPYL5 overexpression, we used a TSPYL5 expression vector in several cellular assays in which the p53-dependent effects on cell proliferation, senescence and transformation

have been well-characterized. In the *ST.HdhQ111* cells, the temperature shift to 39 °C induced a p53-dependent senescence-like arrest¹⁹ (Fig. 4a, b). Stable expression of *TSPYL5* in these cells allowed a bypass of the cell cycle arrest at 39 °C, and continued proliferation was observed. This effect of *TSPYL5* on cell proliferation was shown both in clonogenic assays (Fig. 4a) and in cell proliferation assays (Fig. 4b). Next, we expressed *TSPYL5* in BJ human diploid fibroblasts (HDF) that harboured an inducible *RAS^{V12}* oncogene (*RAS^{V12}-ER*)²². Activation of *RAS^{V12}* by treatment of the cells with 4-hydroxy-tamoxifen (OHT) triggered *RAS^{V12}*-induced senescence, which was effectively prevented by expression of *TSPYL5* (Fig. 4c, d). We also expressed *TSPYL5* in TIG3/16i cells, which are HDF-immortalized by hTERT and have a shRNA targeting *CDKN2A*²³. Acute overexpression of *RAS^{V12}* in TIG3/16i cells resulted in oncogene-induced senescence (OIS), but expression of *TSPYL5* prevented this arrest (Fig. 4e). To further substantiate the effect of *TSPYL5* on OIS, we used a *BRAF^{V600E}* oncogenic allele to induce proliferation arrest in TIG3/16i fibroblasts. *TSPYL5* was able to override the *BRAF^{V600E}*-induced senescence and prevented induction of senescence-associated beta-galactosidase expression in the cells (Fig. 4f). We confirmed that *TSPYL5* was bound to USP7 in TIG3/16i cells before and after the override of *BRAF^{V600E}*-induced senescence (Supplementary Information, Fig. S3a). We used human mammary epithelial cells (HMEC) to investigate if *TSPYL5* could also prevent *RAS^{V12}*-induced senescence in breast epithelium-derived cells. In human mammary epithelial cells (HMECs) harbouring *RAS^{V12}-ER*²⁴, we observed growth arrest and morphological senescence when cells were cultured in media containing tamoxifen. Also in these cells, *TSPYL5* conferred resistance to *RAS^{V12}*-induced senescence and allowed continued proliferation (Supplementary Information, Fig. S4b).

As a final assay, we assessed the oncogenic potential of *TSPYL5*. We took advantage of the finding that primary human fibroblasts can be transformed by the introduction of a combination of genetic elements: *hTERT*, SV40 small t antigen, *RAS^{V12}*, *CDKN2A* shRNA and *p53* shRNA²⁵. We generated primary human BJ fibroblasts expressing the first four genetic elements, and investigated whether *TSPYL5* could replace *p53* shRNA in this assay. Expression of *TSPYL5* allowed the cells to form colonies in soft agar, which is a hallmark of transformation, albeit with reduced efficiency when compared with cells expressing *p53* shRNA (Fig. 4g). In summary, *TSPYL5* can override senescence-like proliferation arrest and oncogene-induced senescence, as well as contribute to transformation, demonstrating that *TSPYL5* can act as a negative regulator of p53 function.

We identify here *TSPYL5* as a novel protein that physically interacts with USP7 and suppresses p53. Functionally, *TSPYL5* resembles the viral Epstein-Barr nuclear antigen 1 (EBNA1) protein, which also interacts physically with USP7 to suppress p53 function by displacement of p53 from USP7 (refs 26, 27). Similarly to *TSPYL5*, EBNA1 binds to the N-terminus of USP7, which is the domain of USP7 known to interact with p53 (refs 14, 26). Hence, *TSPYL5* and EBNA1 share a common mechanism of competitive binding to the USP7 N-terminus to inactivate p53. That *TSPYL5* phenocopies the effects of the EBNA1 viral oncoprotein is consistent with the oncogene-like activity of *TSPYL5* described here. *TSPYL5* is one of the genes in the 8q22 breast cancer amplicon, and we show that *TSPYL5* is an independent poor prognosis marker in breast cancer. Consistent with this, mutation of *p53* itself is also a predictor of poor prognosis in breast cancer^{28,29}. Based on these observations, it might be predicted that there is an inverse correlation between *TSPYL5* expression

and *TP53* mutation in breast cancer, as overexpression of *TSPYL5* leads to functional *TP53* inactivation in breast cancer. However, in the series of 295 breast tumours we examined, no such correlation was found (data not shown). This may be explained by our finding that RNAi against *TP53* in all assays is more efficient in inhibiting p53 than expression of *TSPYL5* (Figs 3 and 4 and Supplementary Information, Figs S4 and S5). Therefore, a continued selection pressure to mutate *TP53* may persist in breast cancer cells, even in tumours with high *TSPYL5* expression. Moreover, binding of *TSPYL5* to USP7 may affect other proteins that are regulated by USP7. A recent study of *Usp7* *in vivo* indicates that regulation of p53 is an important, albeit not the only, function of *Usp7* (ref. 30). *Usp7*-knockout mice die during early embryonic development between embryonic days E6.5 and E7.5, and *Usp7*-knockout embryos show p53 activation. However, concomitant deletion of *p53* only partially rescues the developmental phenotype in *Usp7*-knockout embryos, as *Usp7;p53* double knockout embryos are still embryonic lethal³⁰. This result is also consistent with the notion that *Usp7* has additional targets besides p53.

Finally, there may be an additional selective advantage of 8q22 genomic gain in breast cancer, as this region also harbours *metadherin* (*MTDH*), a gene that mediates metastasis and chemoresistance³, and the genes *LAPTM4B* and *YWHAZ*, which contribute to chemotherapy resistance². The presence of these genes in the same amplified region provides a plausible explanation for the higher risk of clinical progression associated with the presence of this amplicon.

METHODS

Methods and any associated references are available in the online version of the paper at <http://www.nature.com/naturecellbiology/>

Note: Supplementary Information is available on the Nature Cell Biology website

ACKNOWLEDGEMENTS

We thank C. Bishop and D. Beach for the gift of HMEC cells with inducible *RAS^{V12}* and members of the Bernards and Pandolfi laboratories for discussions and critical reading of the manuscript. This work was supported by grants from the Dutch Cancer Society and the Netherlands Genomics Initiative to R.B., by grants from the Netherlands Proteomics Centre and the Netherlands Genomics Initiative to J.L.B. and by NIH grants to P.P.P.

AUTHOR CONTRIBUTIONS

The experiments were conceived and designed by M.T.E., P.P.P. and R.B. Experiments were performed by M.T.E. Mass spectrometry was performed by L.A.T.M. and supervised by J.L.B. Statistical analysis of gene expression in breast cancer was performed by O.K. The paper was written by M.T.E., P.P.P. and R.B.

COMPETING FINANCIAL INTERESTS

The authors declare that they have no competing financial interests.

Published online at <http://www.nature.com/naturecellbiology>

Reprints and permissions information is available online at <http://npg.nature.com/reprintsandpermissions/>

- van 't Veer, L. J. *et al.* Gene expression profiling predicts clinical outcome of breast cancer. *Nature* **415**, 530–536 (2002).
- Li, Y. *et al.* Amplification of *LAPTM4B* and *YWHAZ* contributes to chemotherapy resistance and recurrence of breast cancer. *Nat. Med.* **16**, 214–218 (2010).
- Hu, G. *et al.* *MTDH* activation by 8q22 genomic gain promotes chemoresistance and metastasis of poor-prognosis breast cancer. *Cancer Cell* **15**, 9–20 (2009).
- Li, M. *et al.* Deubiquitination of p53 by HAUSP is an important pathway for p53 stabilization. *Nature* **416**, 648–653 (2002).
- Vousden, K. H. & Lane, D. P. p53 in health and disease. *Nat. Rev. Mol. Cell Biol.* **8**, 275–283 (2007).
- Vogelstein, B., Lane, D. & Levine, A. J. Surfing the p53 network. *Nature* **408**, 307–310 (2000).
- Riley, T., Sontag, E., Chen, P. & Levine, A. Transcriptional control of human p53-regulated genes. *Nat. Rev. Mol. Cell Biol.* **9**, 402–412 (2008).
- Brooks, C. L. & Gu, W. p53 ubiquitination: Mdm2 and beyond. *Mol. Cell* **21**, 307–315 (2006).

9. van de Vijver, M. J. *et al.* A gene-expression signature as a predictor of survival in breast cancer. *N. Engl. J. Med.* **347**, 1999–2009 (2002).
10. Paik, S. *et al.* A multigene assay to predict recurrence of tamoxifen-treated, node-negative breast cancer. *N. Engl. J. Med.* **351**, 2817–2826 (2004).
11. Ma, X. J. *et al.* A two-gene expression ratio predicts clinical outcome in breast cancer patients treated with tamoxifen. *Cancer Cell* **5**, 607–616 (2004).
12. Sorlie, T. *et al.* Gene expression patterns of breast carcinomas distinguish tumor subclasses with clinical implications. *Proc. Natl Acad. Sci. USA* **98**, 10869–10874 (2001).
13. Fan, C. *et al.* Concordance among gene-expression-based predictors for breast cancer. *N. Engl. J. Med.* **355**, 560–569 (2006).
14. Hu, M. *et al.* Crystal structure of a UBP-family deubiquitinating enzyme in isolation and in complex with ubiquitin aldehyde. *Cell* **111**, 1041–1054 (2002).
15. Li, M., Brooks, C. L., Kon, N. & Gu, W. A dynamic role of HAUSP in the p53-Mdm2 pathway. *Mol. Cell* **13**, 879–886 (2004).
16. Cummins, J. M. *et al.* Tumour suppression: disruption of HAUSP gene stabilizes p53. *Nature* **428**, doi:10.1038/nature02501 (2004).
17. Vassilev, L. T. *et al.* *In vivo* activation of the p53 pathway by small-molecule antagonists of MDM2. *Science* **303**, 844–848 (2004).
18. Scheffner, M., Huibregtse, J. M., Vierstra, R. D. & Howley, P. M. The HPV-16 E6 and E6-AP complex functions as a ubiquitin-protein ligase in the ubiquitination of p53. *Cell* **75**, 495–505 (1993).
19. Brummelkamp, T. R. *et al.* TBX-3, the gene mutated in Ulnar-Mammary Syndrome, is a negative regulator of p19ARF and inhibits senescence. *J. Biol. Chem.* **277**, 6567–6572 (2002).
20. Sherr, C. J. Divorcing ARF and p53: an unsettled case. *Nat. Rev. Cancer* **6**, 663–673 (2006).
21. Flatt, P. M. *et al.* p53-dependent expression of PIG3 during proliferation, genotoxic stress, and reversible growth arrest. *Cancer Lett.* **156**, 63–72 (2000).
22. Voorhoeve, P. M. *et al.* A genetic screen implicates miRNA-372 and miRNA-373 as oncogenes in testicular germ cell tumors. *Cell* **124**, 1169–1181 (2006).
23. Kuilman, T. *et al.* Oncogene-induced senescence relayed by an interleukin-dependent inflammatory network. *Cell* **133**, 1019–1031 (2008).
24. Borgdorff, V. *et al.* Multiple microRNAs rescue from Ras-induced senescence by inhibiting p21(Waf1/Cip1). *Oncogene* **29**, 2262–2271 (2010).
25. Voorhoeve, P. M. & Agami, R. The tumor-suppressive functions of the human *INK4A* locus. *Cancer Cell* **4**, 311–319 (2003).
26. Holowaty, M. N., Sheng, Y., Nguyen, T., Arrowsmith, C. & Frappier, L. Protein interaction domains of the ubiquitin-specific protease, USP7/HAUSP. *J. Biol. Chem.* **278**, 47753–47761 (2003).
27. Saridakis, V. *et al.* Structure of the p53 binding domain of HAUSP/USP7 bound to Epstein-Barr nuclear antigen 1 implications for EBV-mediated immortalization. *Mol. Cell* **18**, 25–36 (2005).
28. Pharoah, P. D., Day, N. E. & Caldas, C. Somatic mutations in the *p53* gene and prognosis in breast cancer: a meta-analysis. *Br. J. Cancer* **80**, 1968–1973 (1999).
29. Miller, L. D. *et al.* An expression signature for p53 status in human breast cancer predicts mutation status, transcriptional effects and patient survival. *Proc. Natl Acad. Sci. USA* **102**, 13550–13555 (2005).
30. Kon, N. *et al.* Inactivation of HAUSP *in vivo* modulates p53 function. *Oncogene* **29**, 1270–1279 (2010).

METHODS

Patient data and statistical analysis. Tumours from 295 women with primary invasive breast cancer were selected from the fresh-frozen tissue bank of the Netherlands Cancer Institute (NKI) and used for microarray analysis as described previously⁹. All microarray data and patient data can be downloaded at: <http://bioinformatics.nki.nl/data.php>. Study design, patient selection, RNA isolation from tumour material, histopathological analyses, clinical annotation and clinical interpretation were as described⁹. *TSPYL5* expression was qualified as the log₂ intensity ratio with respect to a standard pool of breast cancers. Cut-off determination was performed using a random split of the series into a training set and a validation set. Using the training set we determined the expression level of *TSPYL5* that yielded the largest difference in survival between the *TSPYL5*^{high} and *TSPYL5*^{low} groups. To evaluate the prognostic value of *TSPYL5* expression we performed univariate Kaplan–Meier analysis using the logrank test in the statistical programming language R, version 2.11.1 and the Bioconductor ‘Survival’ package³¹. P-values < 0.05 were considered significant.

Plasmids, reagents and antibodies. *TSPYL5* cDNA was generated by PCR from a human breast tumour cDNA pool and cloned, resulting in the plasmids pcDNA3.1-TSPYL5 and pCR3-CMV-Flag-TSPYL5. The pBabePuro retroviral vector was modified to express N-terminal tags for tandem affinity purification of TSPYL5. The biotinyl tag MASSLRQLDSQKMEWRSNAGGS³² was cloned into pBabePuro and three Flag tags were added to the *Bam*HI site upstream of the biotinyl tag to generate the empty vector. *TSPYL5* was cloned into the *Eco*RI site downstream of the tags, resulting in the pBabePuro-3 × Flag-Nbio-TSPYL5 retroviral plasmid. The BirA biotin ligase was cloned into MSCVneo. MCF7 cells were infected with both retroviruses and selected in puromycin and neomycin, and these cells were used for TSPYL5 protein purification. The Myc-USP7 construct was a gift from B. Burgering (Utrecht University, Netherlands). Plasmids encoding USP7 domains were generated by PCR and cloned into the pEGFP vector. Flag-p53 and Flag-MDM2 were generated by cloning the respective cDNAs into pCR3-CMV-Flag. The siRNA pools specific to TSPYL5 and USP7 were purchased from Dharmacon. *TSPYL5* siRNA target sequences were: 5'-GUACUGAGCUACUU-AAACA-3', 5'-GAUAAUCAACGAAAUUG-3', 5'-GAUAUUGGGUGUGGUCCUU-3' and 5'-CAGCUAGCAUCCUUUCUGA-3'. *USP7* siRNA target sequences were: 5'-CUAAGGACCCUGCAAUUA-3', 5'-GUGGUUACGUUAUCAAUA-3', 5'-UGACGUGUCUUGAUAAA-3' and 5'-GAAGGUACUUUAAGAGAUC-3'. The target sequence in the pRetroSuper-p53 shRNA vector against human p53 was 5'-GACTCCAGTGGTAATCTAC-3' and against mouse p53 was 5'-GTACATGTGTAATAGCTCC-3'. In the pRetroSuper-MDM2 shRNA vector the target sequence against MDM2 was 5'-GATGATGAGGTATATCAAG-3'. The proteasome inhibitor MG132 (CBZ-LLL) and 4-hydroxy-tamoxifen were obtained from Sigma and Nutlin-3 was purchased from Cayman Chemical. MG132 was used at 10 μM final concentration for 4–6 h. Antibodies against p53 (DO-1; 1:1,000), p21CIP (F5; 1:1,000), GADD45A (H-165; 1:1,000), Bax (N-20; 1:1,000), Myc (9E10; 1:1,000), TSPYL5 (N-15; 1:400), MDM2 (SMP14; 1:500), PCNA (PC10; 1:1,000), HSP90α/β (H-114; 1:1,000) and α-tubulin (TU-02; 1:1,000) were from Santa Cruz Biotechnology. The USP7 antibody (1:4,000) was from Bethyl Laboratories, the p19ARF antibody (1:1,000) was from Abcam, the HA (16B12; 1:1,000) antibody was from Covance, the GFP antibody was from Invitrogen (1:1,000), the PARP antibody (46D11; 1:1,000) was from Cell Signaling, and the antibodies against Flag (M2) (1:4,000) and actin (1:4,000) were from Sigma.

Protein purification and mass spectrometry. MCF7 cells were lysed in lysis buffer (50 mM Tris at pH 7.5, 10% glycerol, 5 mM MgCl₂, 75 mM NaCl, 0.2% NP-40, protease inhibitor cocktail EDTA-free (Complete, Roche), 10 mM NaF, 0.2 mM Na₃VO₄, 2.5 mM sodium pyrophosphate and 2.5 mM sodium β-glycerophosphate) for 30 min and the lysates were centrifuged and incubated with anti-Flag M2 affinity gel (Sigma). The immunoprecipitates were washed with wash buffer (50 mM Tris at pH 7.5, 5 mM MgCl₂, 75 mM NaCl, 0.1% NP-40, protease inhibitor cocktail EDTA-free (Complete, Roche), 10 mM NaF, 0.2 mM Na₃VO₄, 2.5 mM sodium pyrophosphate and 2.5 mM sodium β-glycerophosphate) and eluted using 160 ng μl⁻¹ 3 × Flag peptide (Sigma) in wash buffer. The eluates were incubated with streptavidin magnetic beads (NEB) and the precipitates were washed with wash buffer, eluted in Laemmli sample buffer and separated on Bis-Tris gradient gels (NuPAGE Novex, Invitrogen). The gels were stained with SimplyBlue Safe Stain (Invitrogen) and whole gel lanes were excised, sliced into smaller pieces and

subjected to in-gel trypsinization followed by LC–MS/MS analysis.

Immunoprecipitation and western blotting. For immunoprecipitation, cells were lysed as described above for protein purification and the lysates were incubated with anti-Flag M2 affinity gel (Sigma). After washing with wash buffer, the immunoprecipitates were separated on 9% SDS–PAGE (sodium dodecyl sulfate polyacrylamide gel electrophoresis) gels. Proteins were transferred to polyvinylidene difluoride membranes (Immobilon P, Millipore) and the blots were probed with the indicated antibodies. Immunoprecipitations of p53 and USP7 were performed using IP buffer (50 mM Tris at pH 7.5, 150 mM NaCl, 0.1% NP-40, 1 mM EDTA and a protease inhibitor cocktail; Complete, Roche). For western blotting, cells were lysed in Ripa buffer (50 mM Tris at pH 8.0, 150 mM NaCl, 1% NP-40, 0.5% deoxycholic acid, and 0.1% SDS) supplemented with protease inhibitors (Complete, Roche).

Cell culture and luciferase assays. All cells were cultured in DMEM (Dulbecco's Modified Eagle Medium) supplemented with 10% fetal calf serum (FCS) and maintained at 37 °C, except for ST.HdhQ111 cells, which were maintained at 32 °C or 39 °C as indicated. ST.HdhQ111 cells are mouse neuronal cells that harbour a temperature-sensitive mutant of the SV40 Large T (LT) oncogene¹⁹. BJ-RAS^{V12}-ER cells contained an MSCVBlast-RAS^{V12}-ER fusion construct that was activated by treatment of cells with 4-hydroxy-tamoxifen (OHT)²². TIG3/16i fibroblasts were immortalized by expression of *hTERT* and contained a *CDKN2A* shRNA construct, as described²³. BJ or TIG3/16i cells were infected with TSPYL5 retrovirus and subsequently with MSCVBlast-RAS^{V12} or MSCVBlast-BRAF^{V600E} retrovirus and selected in blasticidin. HMEC cells harbouring RAS^{V12}-ER were cultured in serum-free MEGM medium (Lonza) and senescence was induced on treatment with tamoxifen²⁴. Retroviral supernatants were generated by transfection of Phoenix packaging cells with retroviral plasmids.

For reporter assays, U2OS cells were transfected with 0.5 μg of reporter-luciferase, 10 ng CMV-renilla and 3 μg of the indicated expression plasmids using calcium phosphate precipitation. The indicated ligands were added 48 h after transfection and assays were done 72 h after transfection. Normalized luciferase activities shown represent ratios (mean ± s.d. of triplicates) between firefly luciferase values and renilla luciferase internal control values and were measured using the dual reporter luciferase assay system (Promega).

Quantitative RT-PCR. Total RNA was extracted using the Trizol reagent (Invitrogen) and 1 μg RNA was used to prepare first-strand cDNA using the SuperScriptII polymerase (Invitrogen). Quantitative real-time PCR reactions were performed using SYBR Green master mix (Applied Biosystems) in the 7500 Fast Real-Time PCR System (Applied Biosystems). Relative mRNA levels of each gene shown were normalized to the expression of the housekeeping genes *GAPDH* or *β-Actin*.

List of the primers used for quantitative PCR: *TSPYL5* fwd: 5'-GCCAGCTC-TGCTTTTACAC-3', *TSPYL5* rev: 5'-GCATCTCAAGCTTCTCCTGG-3'; *Actin B* fwd: 5'-CCTGGCACCAGCACAA-3', *Actin B* rev: 5'-GCCATCCACACGGAGTACT-3'; *GAPDH* fwd: 5'-AAGGTGAAGGTCGGAGTCAA-3', *GAPDH* rev: 5'-AATGAAGGGGTCATTGATGG-3'; *p53* fwd: 5'-GCTTTCCAC-GACGGTGAC-3', *p53* rev: 5'-GCTCGACGCTGAGTATCTGAC-3'; *CDKN1A* (p21) fwd: 5'-TGCGTTCACAGGTGTTCTG-3', *CDKN1A* (p21) rev: 5'-GTCCACTGG-CGCCAAGAG-3'; *GADD45A* fwd: 5'-GAGAGCAGAAGACCGAAAGGA-3', *GADD45A* rev: 5'-CACAAACCACGTTATCGGG-3'; *MDM2* fwd: 5'-GGCAGGG-GAGAGTGATACAGA-3', *MDM2* rev: 5'-GAAGCCAATTCTCACGAAGGG-3'. Mouse genes: *Cdkn1A* (p21) fwd: 5'-CCTGGTGATGTCGACCTG-3', *Cdkn1A* (p21) rev: 5'-CCATGAGCGCATCGAATC-3'; *Btg2* fwd: 5'-ATGAGC-CACGGGAAGAGAAC-3', *Btg2* rev: 5'-GCCCTACTGAAAACCTTGAGTC-3'; *Bax* fwd: 5'-TGAAGACAGGGGCCTTTTG-3', *Bax* rev: 5'-AATTCGCGGA-GACTCG-3'; *Noxa* fwd: 5'-GCAGAGCTACCACCTGAGTTC-3', *Noxa* rev: 5'-CTTTTGGGACTTCCCAGGCA-3'; *Mdm2* fwd: 5'-GGCAGGGGAGAGTG-ATACAGA-3', *Mdm2* rev: 5'-TCCAACGGACTTAAACAACCTTCA-3'; *Actin B* fwd: 5'-GGCTGTATTCCCTCCATCG-3', *Actin B* rev: 5'-CCAGTTGGTAACAA-TGCCATGT-3'.

31. Gentleman, R. C. *et al.* Bioconductor: open software development for computational biology and bioinformatics. *Genome Biol.* **5**, R80 (2004).

32. de Boer, E. *et al.* Efficient biotinylation and single-step purification of tagged transcription factors in mammalian cells and transgenic mice. *Proc. Natl Acad. Sci. USA* **100**, 7480–7485 (2003).

DOI: 10.1038/ncb2142

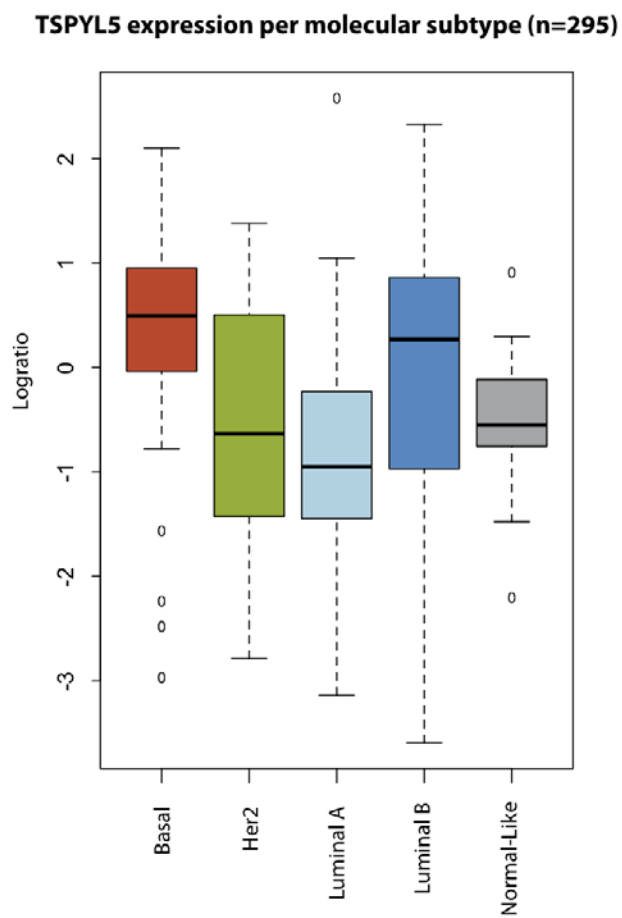


Figure S1 TSPYL5 expression in breast cancer molecular subtypes. Boxplot showing TSPYL5 expression in five molecular subtypes of breast cancer (N=295 patients)¹³.

SUPPLEMENTARY INFORMATION

```

1  MNHQQQQQQQ KAGEQQQSEP EDMEMEAGDT DDPPRITQNP VINGNVALSD GHNTAEEDME
61  DDTSWRSEAT FQFTVERFSR LSESVLSPPC FVRNLPWKIM VMPRFYPPDRP HQKSVGFFLQ
121 CNAESDSTSW SCHAQAVLKI INYRDDEKSF SRRISHLFFH KENDWGFSNF MAWSEVTDPE
181 KGFIDDDKVT FEVQVADAP HGVAVDSKKH TGYVGLKNQG ATCYMNSLLQ TLFFFTNQLRK
241 AVYMPTEGD DSSKSVPLAL QRVFYELQHS DKPVGTKKLT KSFGWETLDS FMQHDVQELC
301 RVLLDNVENK MKGTCVEGTI PKLFRGKMVS YIQCKEVDYR SDRREDDYDI QLSIKGKKNI
361 FESFVDYVAV EQLDGDNKYD AGEHGLQEA EKVKFLTLPP VLHLQLMRFM YDPQTDQNIK
421 INDRFEFPEQ LPLDEFLQKT DPKDPANYIL HAVLVHSGDN HGGHYVVYLN PKGDGKWCKF
481 DDDVVSRCTK EEAIEHNYGG HDDL SVRHC TNAYMLVYIR ESKLSEVLQA VTDHDI PQQL
541 VERLQEEKRI EAQKRKERQE AHLYMQVQIV AEDQFCGHQG NDMYDEEKVK YTVFKVLKNS
601 SLAEFVQSLS QTMGFQDQI RLWPMQARSN GTRPAMLDN EADGNKTMIE LSDNENPWTI
661 FLETVDPELA ASGATLPKFD KDHDVMLFLK MYDPKTRSLN YCGHIYTPIS CKIRDLLPVM
721 CDRAGFIQDT SLILYEEVKP NLTERIQDYD VSLDKALDEL MDGDIIVFQK DDPENDNSEL
781 PTAKEYFRDL YHRVDVIFCD KTIPNDPGFV VTLSNRMNYF QVAKTVAQRL NTDPMLLQFF
841 KSQGYRDGPG NPLRHNYEGT LRDLLQFFKP RQPKKLYYQQ LKMKITDFEN RRSFKCIWLN
901 SQFREEEITL YPDKHGCVRD LLEECKKAVE LGEKASGKLR LLEIVSYKII GVHQEDELLE
961 CLSPATSRTF RIEEIPLDQV DIDKENEMLV TVAHFHKEVF GTFGIPFLLR IHQGEHFREV
1021 MKRIQSLLDI QEKEFEKFKF AIVMMGRHQY INEDEYEVNL KDFEPQPGNM SHPRPWLGLD
1081 HFNKAPKRSR YTYLEKAIKI HN

```

Figure S2 Identification of USP7 as a TSPYL5-interacting protein. Amino acid sequence of USP7 with the seven unique peptides identified by LC-MS/MS in TSPYL5-containing complexes highlighted in grey.

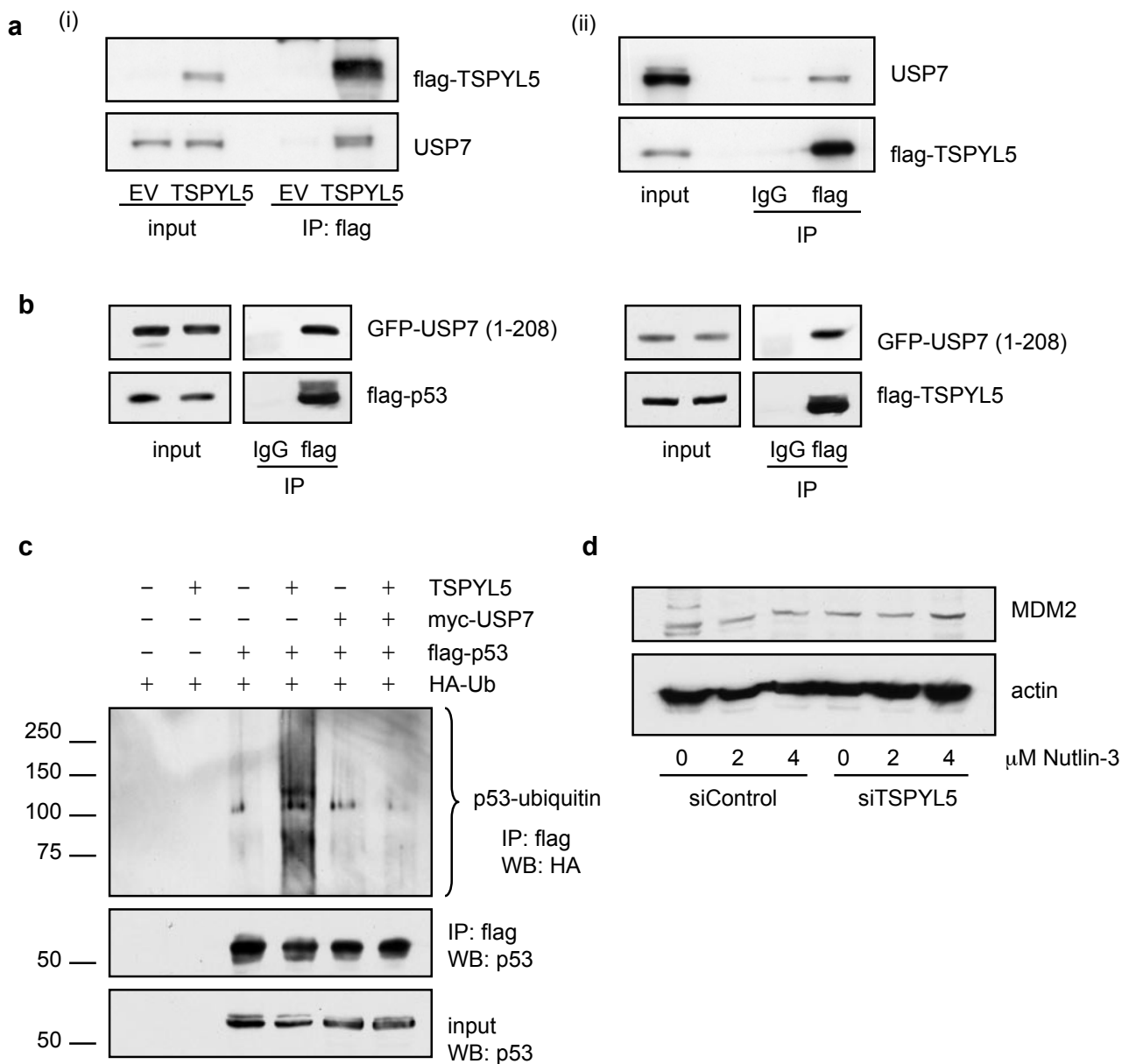


Figure S3 Interaction between TSPYL5 and USP7. **a**, Western blot analysis of TSPYL5 immunoprecipitates (IP) from TIG3/16i human fibroblasts (i) and TIG3/16i cells expressing BRAF^{V600E} that had been rescued from oncogene-induced senescence by expression of TSPYL5 (ii), as shown in Fig. 4f. **b**, Lysates of 293 cells transfected with GFP-USP7 (1-208) and either flag-p53 or flag-TSPYL5 were immunoprecipitated with anti-flag antibody and analysed by western blotting. Both p53 and TSPYL5 interacted

with the N-terminus of USP7. **c**, 293 cells transfected with flag-p53, HA-ubiquitin and TSPYL5 or USP7 were analysed for ubiquitination after treatment with MG132 by immunoprecipitation using an anti-flag antibody and western blotting with an anti-HA antibody. **d**, MCF7 cells transfected with TSPYL5 siRNA were treated with Nutlin-3 for 24 hrs and the lysates were immunoblotted for MDM2. Uncropped images of blots are shown in Supplementary Information, Fig. S6.

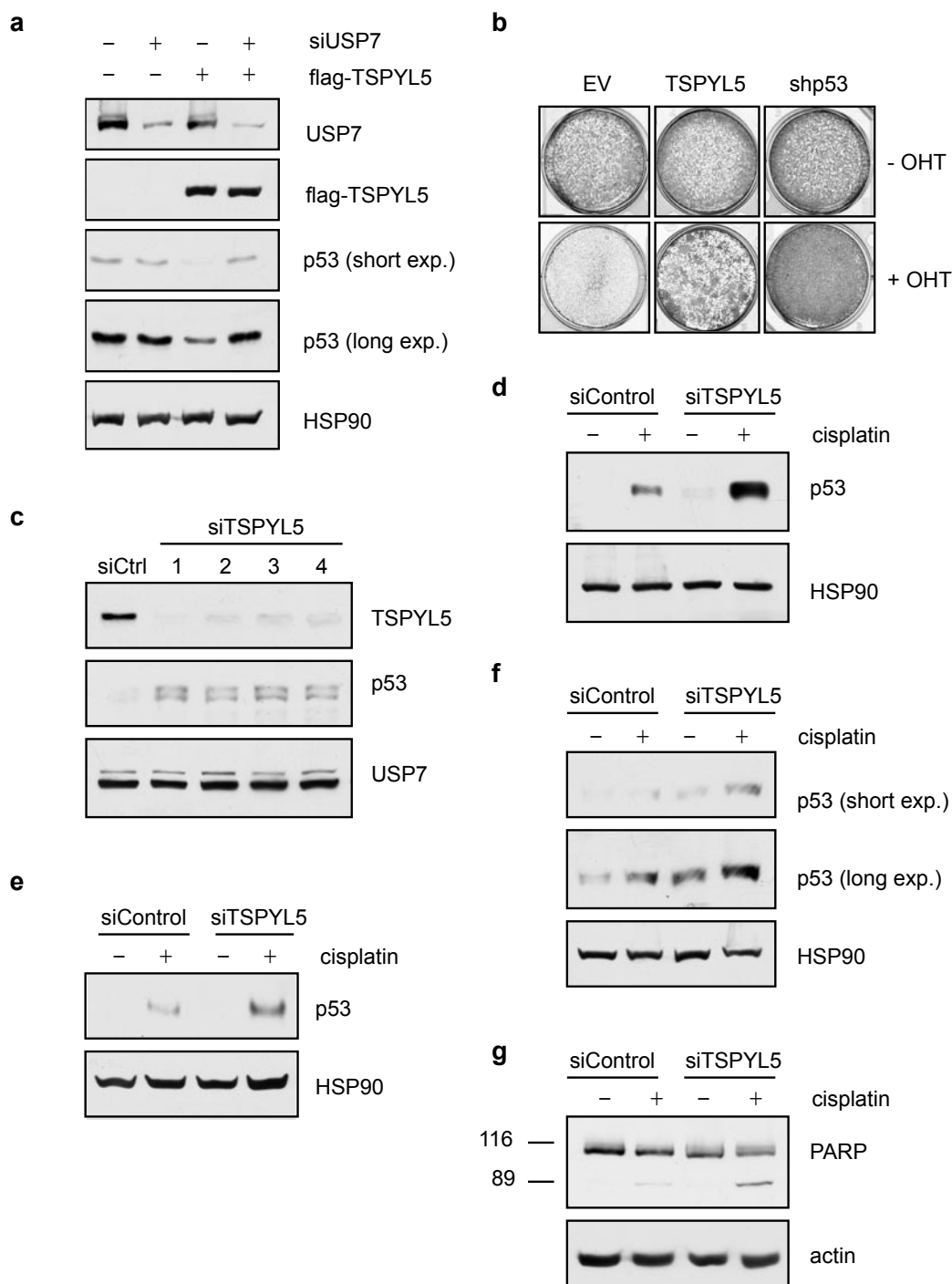


Figure S4 Regulation of p53 levels by TSPYL5 is USP7-dependent. **a**, The effect of TSPYL5 on p53 levels in U2OS cells was tested in the presence of USP7 RNAi. The cells were treated with cisplatin (4 μ g/ml) to stabilize p53 prior to immunoblotting for p53, USP7, flag-TSPYL5 and HSP90. **b**, HMEC cells with stable expression of RAS^{V12}-ER were infected with empty vector (EV), flag-TSPYL5, or p53 shRNA (shp53) and cultured in the absence or presence of tamoxifen (OHT). **c**, Western blot showing TSPYL5, p53 and

USP7 levels in MCF7 cells transfected with four independent siRNAs against TSPYL5. **d-f**, MCF7 (**d**) ZR75-1 (**e**) and HeLa (**f**) cells were transfected with TSPYL5 siRNA and treated with cisplatin (4 μ g/ml) for 24 hrs prior to immunoblotting for p53. **g**, MCF7 cells were transfected with TSPYL5 siRNA and treated with cisplatin (10 μ g/ml) for 16 hrs prior to immunoblotting for PARP (116 kDa) and cleaved PARP (89 kDa). Uncropped images of blots are shown in Supplementary Information, Fig. S6.

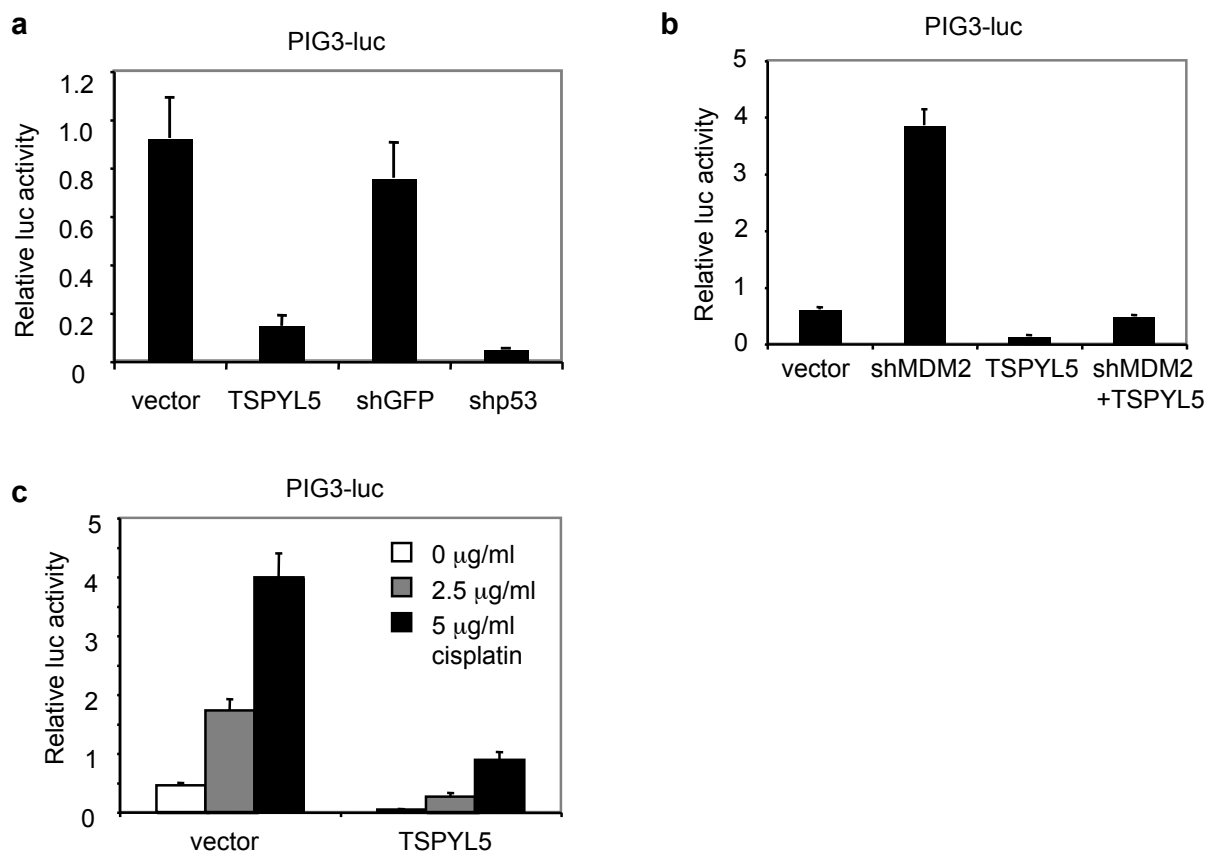


Figure 5 TSPYL5 inhibits p53-dependent transcriptional activation. PIG3-luciferase reporter assays for p53-mediated transactivation in U2OS cells transfected with CMV-TSPYL5 or shRNAs targeting GFP or p53 (a), or MDM2 shRNA (b), or after treatment with cisplatin for 24 hrs (c) (mean \pm s.d.).

Fig. 1d

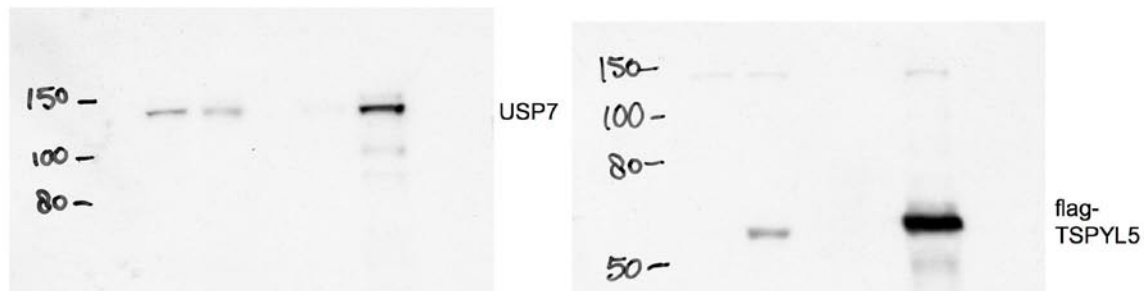


Fig. 1g

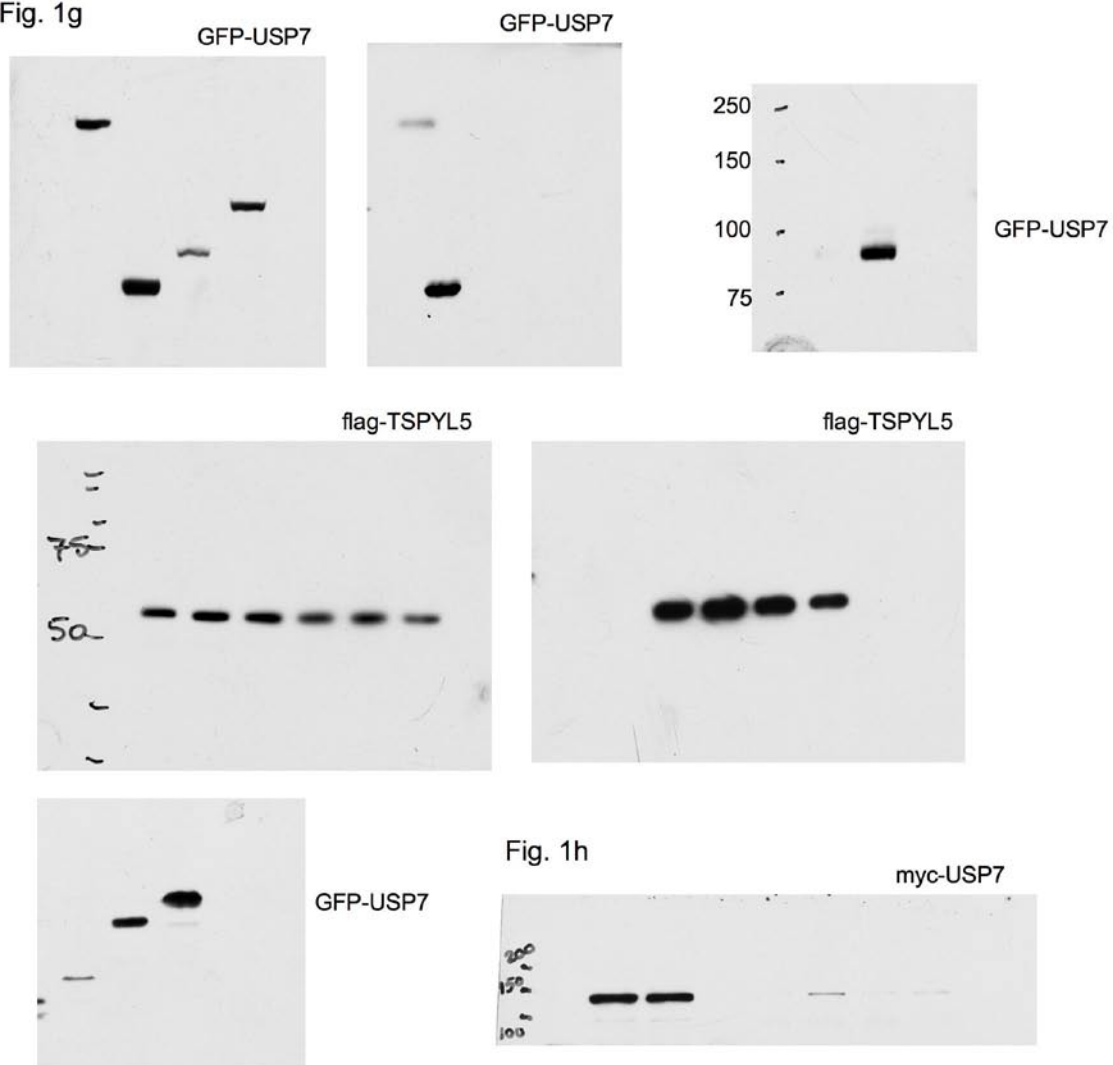


Figure S6 Full scans

Fig. 2b

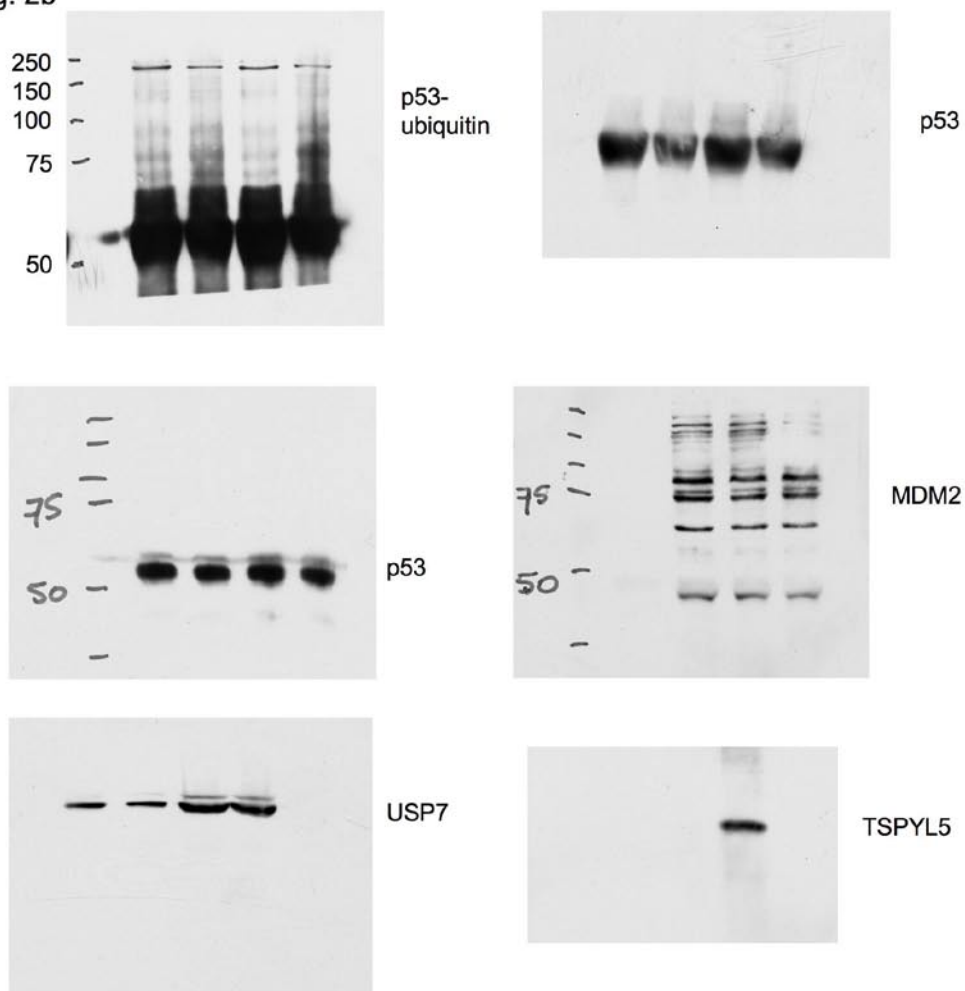


Fig. 2c



Figure S6 continued

Fig. 2d

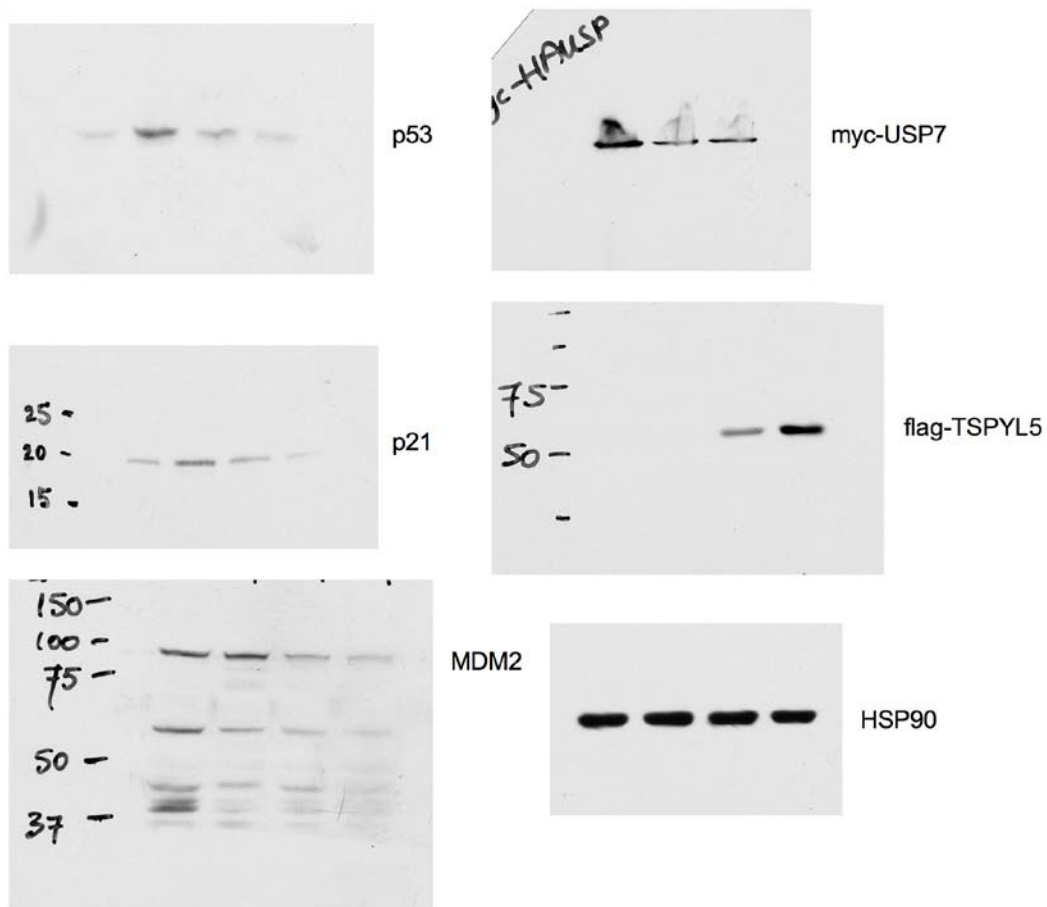


Figure S6 continued

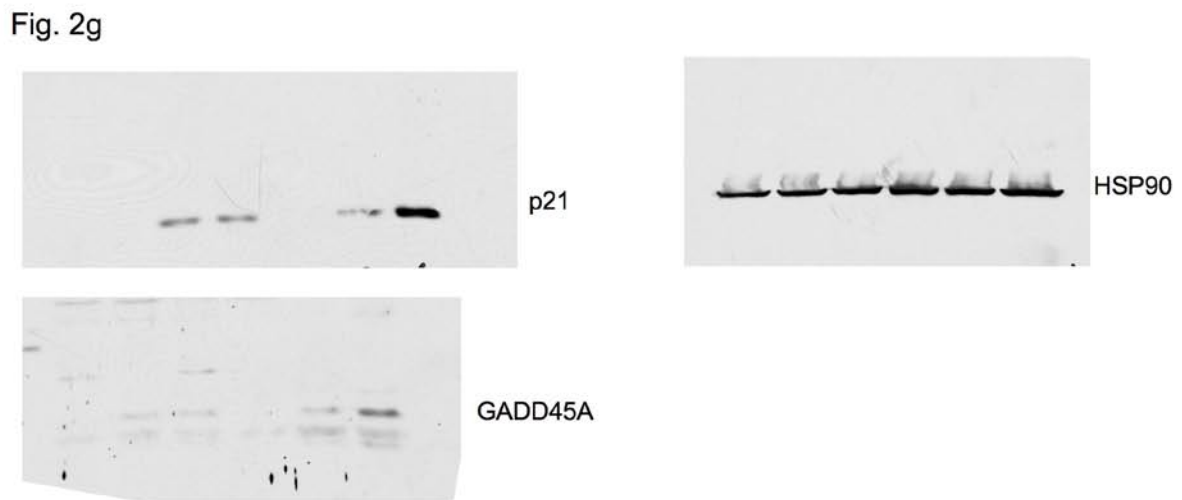
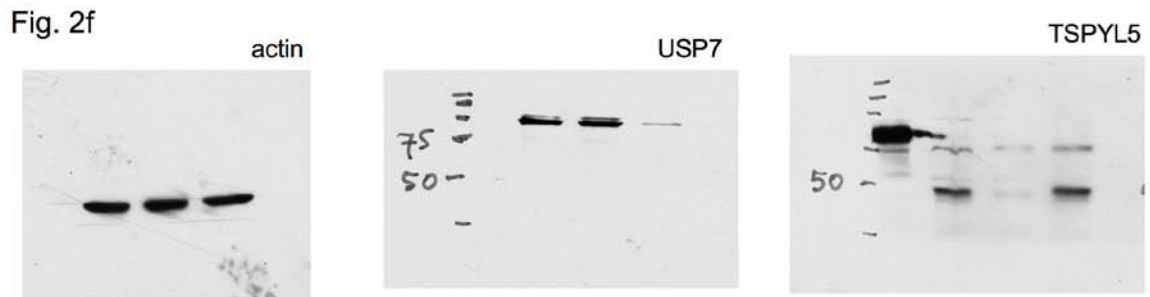


Figure S6 continued

Fig. 3a

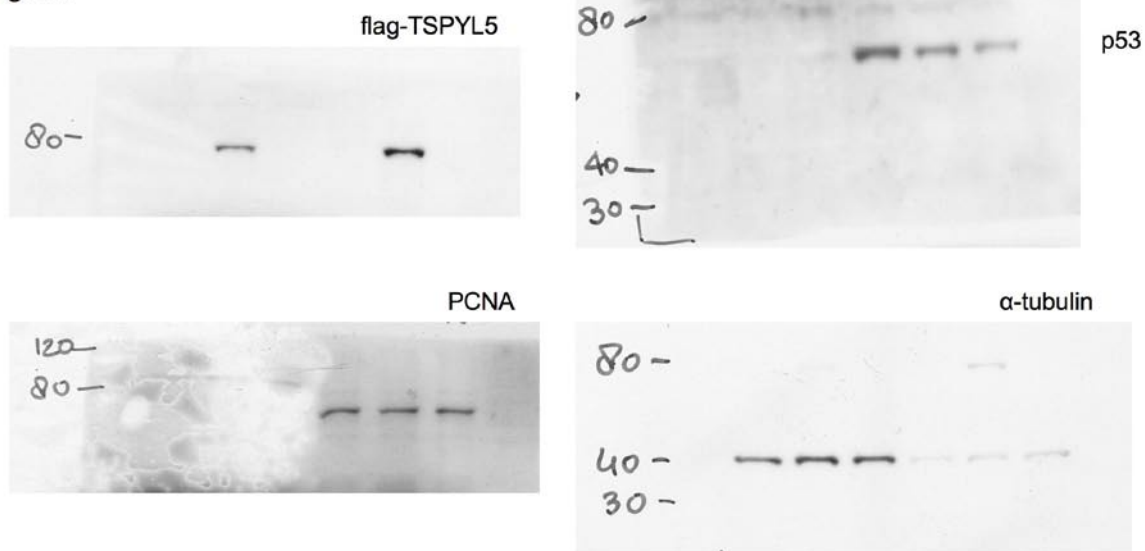


Fig. 3b

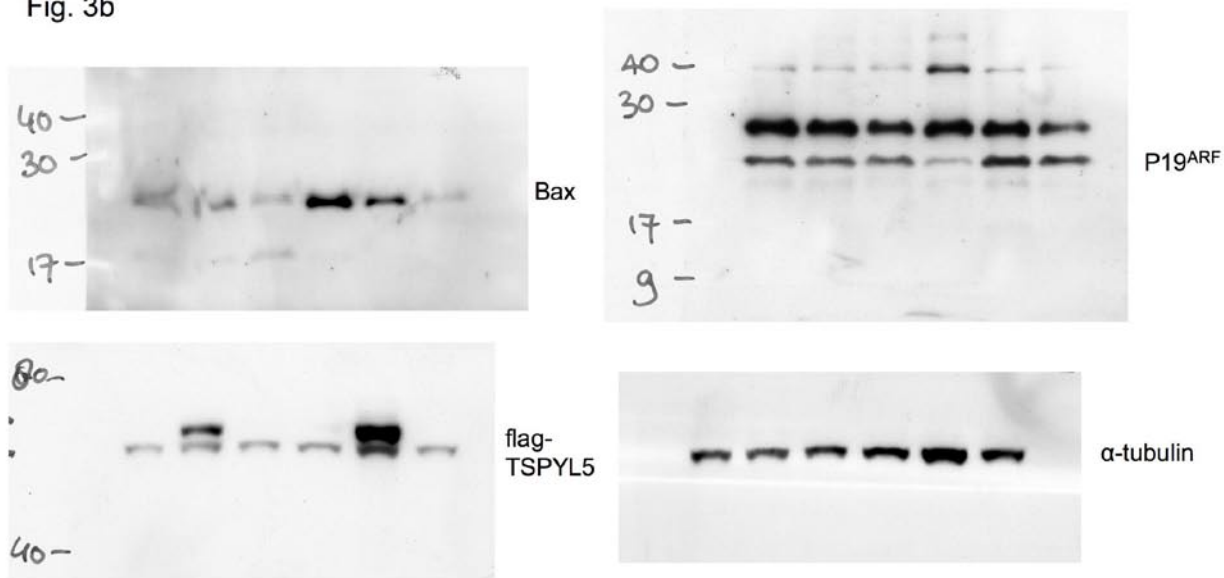


Figure S6 continued

Fig. S3a

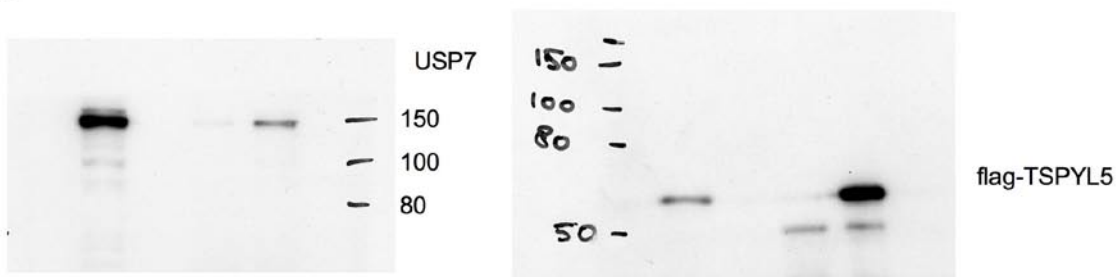


Fig. S3b

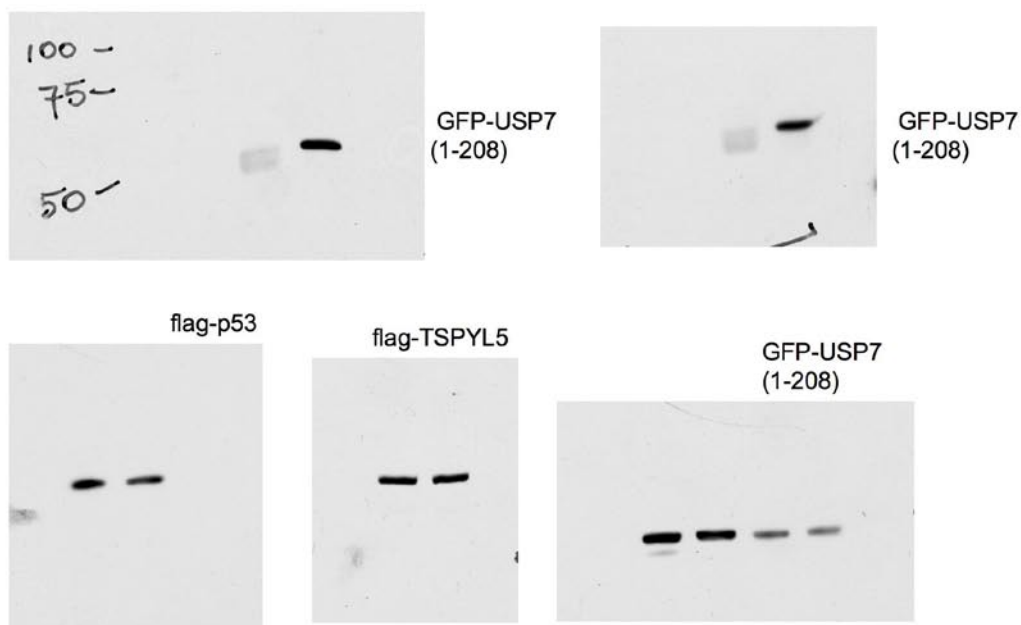


Fig. S3d



Figure S6 continued

Fig. S5a

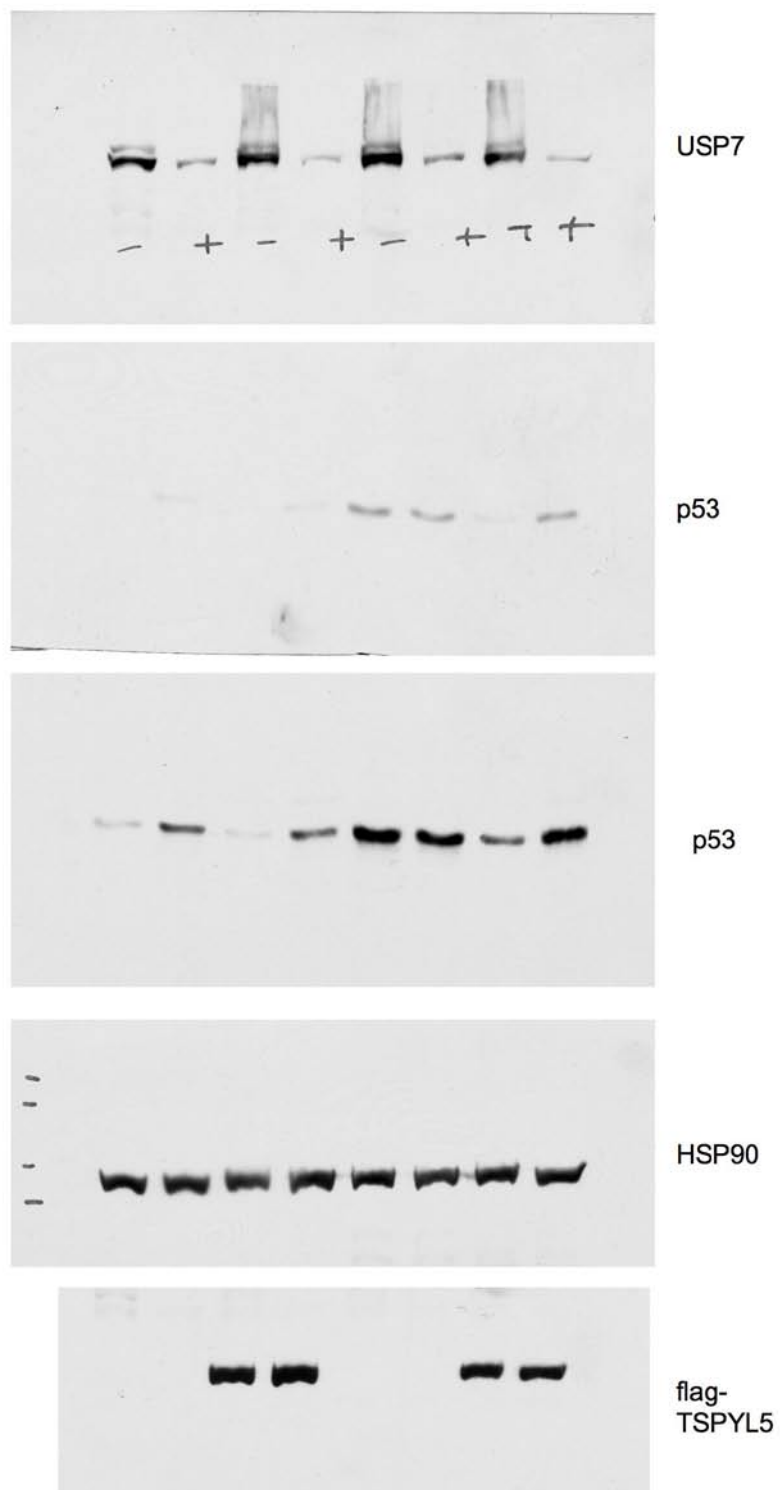


Figure S6 continued

Fig. S5c

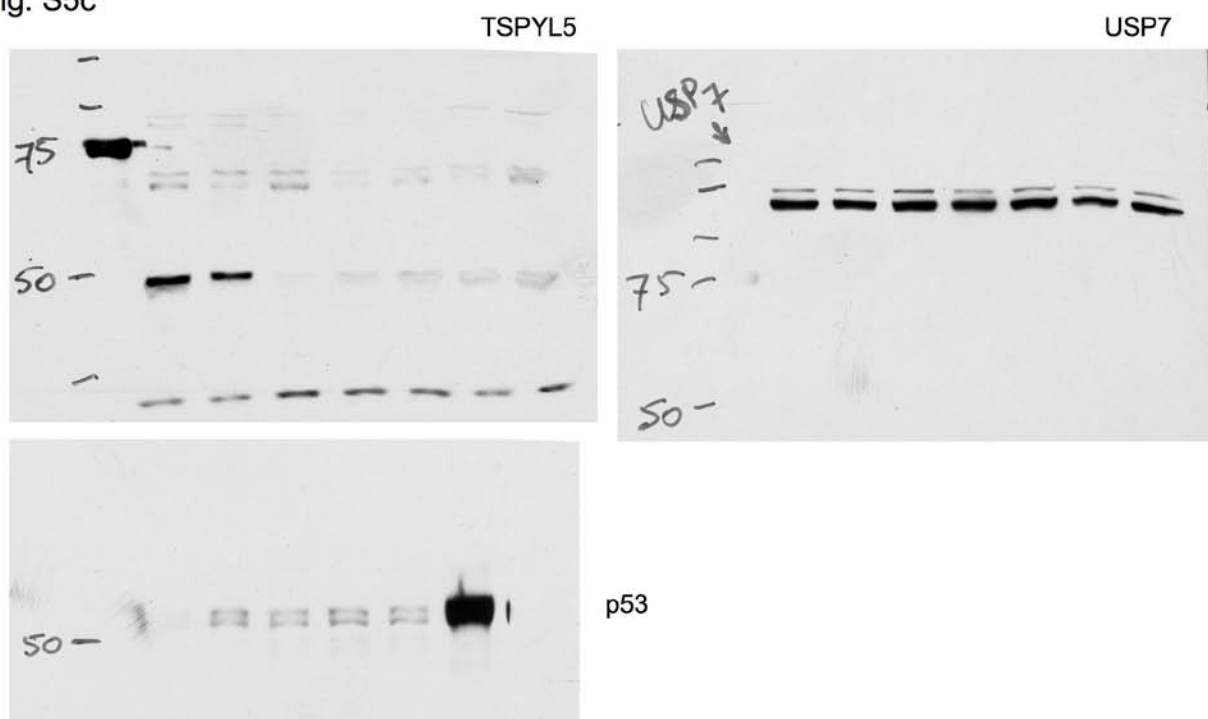


Figure S6 continued

Fig. S5d

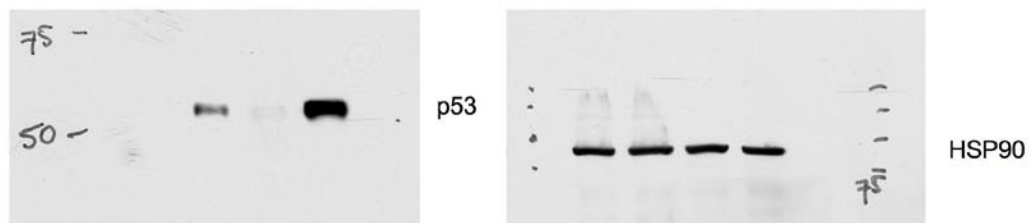


Fig. S5e

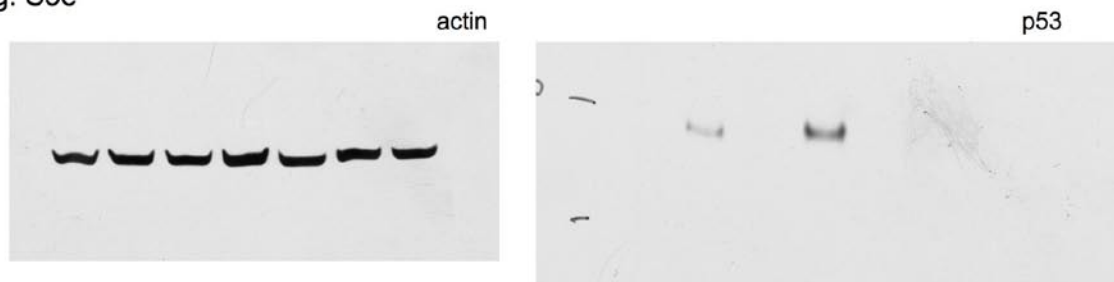


Fig. S5f

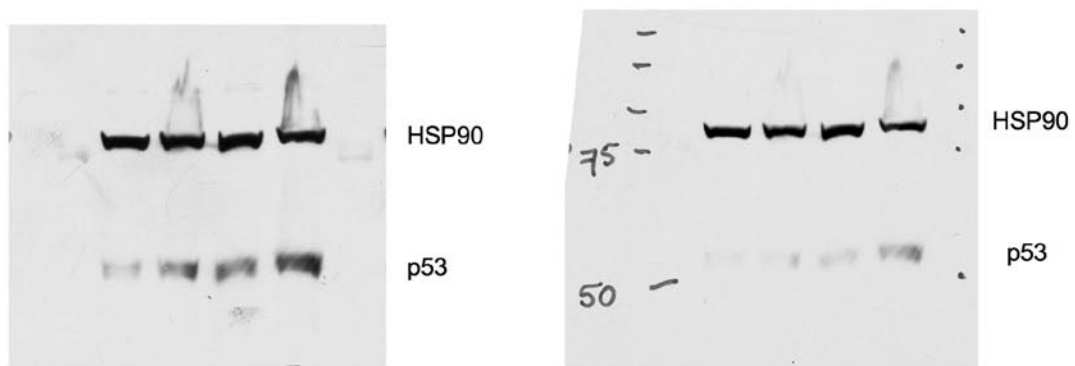


Fig. S5g

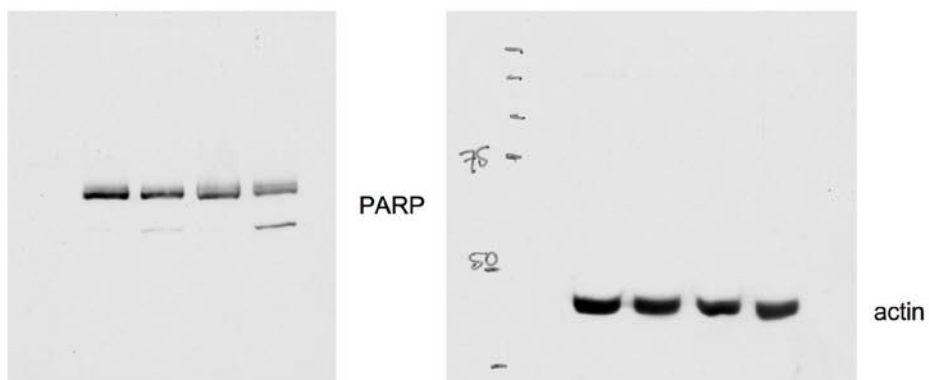


Figure S6 continued